UNIVERSITY OF OKLAHOMA

GRADUATE COLLEGE

SEISMIC DATA REPROCESSING OF A GRANITE WASH SURVEY, BUFFALO WALLOW FIELD, ANADARKO BASIN, TEXAS

A THESIS

SUBMITTED TO THE GRADUATE FACULTY

in partial fulfillment of the requirements for the

Degree of

MASTER OF SCIENCE

By

OLUWATOBI OLORUNSOLA GABRIEL
Norman, Oklahoma
2017

SEISMIC DATA REPROCESSING OF A GRANITE WASH SURVEY, BUFFALO WALLOW FIELD, ANADARKO BASIN, TEXAS

A THESIS APPROVED FOR THE
CONOCOPHILLIPS SCHOOL OF GEOLOGY AND GEOPHYSICS

BY

_____
Dr. Kurt Marfurt, Chair

_____
Dr. Xiaowei Chen

_____
Dr. Bradley Wallet

Note to Self:

Obedience go far!

To Mum & Dad,

The Fighters of my Wars!

To the Future:

Oluwajomiloju & Iremide.

Acknowledgement

When I decided to pursue a graduate degree in Geophysics; it was one met with a conscious unsettling, the unusual kind that puffs along when an unfamiliar task is embarked. But I have certainly graced through the seasons and continue to find depth in knowledge, renewed motivations and guided directions in my everyday learnings of the physics of the Earth.

As I write, I'm reminded of how the journey of a degree at the University of Oklahoma started, and more importantly, the events that shaped how Stephen Ekwunife whom I had only met over phone conversation mentioned me to the graceful Dr. Kurt Marfurt, who would later become my advisor the next year. For that and everything in between, I'm most grateful. Kurt's astuteness, cheer, resourcefulness and patriarchal nurturing are ideals that would continue to be with me forever! Indeed, I have dined with the BEST! – Thank YOU!

My gratitude extends dearly to my thesis supervisory committee, Dr. Bradley Wallet, Dr. Xiaowei Chen and Dr. Jamie Rich. On many occasions, Dr. Brad's 'Tobi, keep up the good work' phrase has a magical way of redeeming a 'bad' day and without a doubt comes with it an instilled sense of hope. I am also very indebted to Dr. Rich, first, for accepting to advise my first year research here at OU and for his mentorship through my entire summer internship at Devon Energy. To those whose technical insights and encouragements saw this project to its deserved completion; Lennon Infante, Thang Ha, 'Mohsen Alali, Rafael Pirés De Lima, 'Lanre Aboaba (University of Arkansas) and Dr. Bode Omoboya (Shell America). I am most grateful!

Many thanks to past and current administrative staff and faculty of the ConocoPhillips School of Geology and Geophysics: Teresa Hackney, Amber Roberts, Rebecca Fay, Ginny Guedes, Dr. Doug Elmore, especially Dr. Randy Keller who is not just the Professor but a man I look up to very dearly! While I have spent most of my time either in class or the Famous-infamous crustal imaging laboratory, I have also enjoyed moments shared with friends who became families whilst here: Ifunanya Ekwunife, Oluwaseyi Ogunsola, Oluseyi Samuel Fadipe, Evangeline Oshenye, Taiwo and Adesuwa Omotoso, Omotola Adewuyi, Feyi Fakoya, Tope Rotimi, Babatunde Babayemi, Chinedum Ezeakacha, Seye Dada and Akinjide Akintunde. These guys are a Joy!

I also want to express my sincere appreciation to Devon Energy for providing the seismic and well data used in this study, Schlumberger for Petrel and Vista Packages, CGG Veritas for Hampson Russell Software. In addition, this degree would not have been attainable without the financial support of all the sponsors of the AASPI Consortium as well as scholarship merits from the Society for Exploration Geophysicists (SEG) and the National Society of Black Geoscientists.

Through my parents and siblings, I have learned the love of God, the appreciation for life, and the desire to succeed. Their selfless giving of love has made me realize the important aspects of life and has made me a better person. For that and all that matters, I am eternally grateful! Finally, without God, all of this will be worthless. To Him I owe this accomplishment!

Table of Contents

List of Tables

List of Figures

Abstract

Although considered one of the more productive oil and gas reservoirs in the United States, the Pennsylvanian-age Granite Wash reservoir remain poorly understood. Amongst a myriad of issues that hinder development of hydrocarbon reserves are unusually low porosity and permeability estimates, varying grain sizes, mineralogy, cementation and the presence of micro-fractures. These heterogeneities not only influence the reservoir performance but have also make the targets difficult to image seismically. To address this later issue, I apply state-of-the-art seismic processing and data conditioning techniques to a 3D seismic volume acquired over the study area. Due to surface conditions overlying this complex play, the seismic data are highly contaminated by coherent and random noise, such as ground-roll, reverberation and air-blast events, resulting in a seismic processing challenge. To improve seismic interpretation, I reprocessed the raw field gathers through coherent noise suppression, prestack Kirchhoff migration, and other sophisticated data conditioning techniques such as spectral-balancing and structured-oriented filtering to improve the quality of the re-processed data.

To understand the reservoir geomorphology and lithological heterogeneity, using seismic geometric, textural attributes and inversion volumes, I construct what I believe to be the first seismic facies analysis of the Desmoinesian-Cherokee wash of Wheeler and Hemphill counties, Texas. An unsupervised latent space Generative Topographic Mapping (GTM) technique provides images of rock-facies types and reservoir quality using facies predictions from a previous well-based study in the same area as ground truth. These facies map provide images of specific alluvial fan depositional environments

and reservoir facies from seismic data as well as identifying productive chaotic facies using these attributes.

Chapter 1: Introduction

Often touted as a complex alternating stack of varying lithologic and depositional patterns, the Granite Wash formation continues to confound experts and operators. Each potential pay zone exhibits a uniquely different reservoir character and as a result requires a slightly different geophysical approach to achieve success (Durrani et. al., 2014). Although considered one of the most productive oil and gas reservoirs in the United States, the Pennsylvanian-age Granite Wash reservoir remain poorly understood. Amongst a myriad of issues that hinder development of hydrocarbon reserves are unusually low porosity and permeability estimates, varying grain sizes, mineralogy, cementation and presence of micro-fractures. These factors have not only influenced its complex stratigraphic and structural depositional pattern but have also made the formation difficult to image seismically (Gillman, 2012; Mitchell, 2012; Sahl, 1970). Hence, understanding the depositional history and the geological variations is critical to drilling and completion strategies.

Straddling the northeastern Pandhandle area of Texas to western Oklahoma, the depositional settings in granite wash reservoirs occur as a series of alluvial fans, debris flows, and fan deltas containing interbedded shales and carbonates (Mitchell, 2011). Alluvial fans generally exhibit complex stratigraphy and constitute some of the world's most productive hydrocarbon reservoirs facies. As a result, a clear understanding of the architectural and facies relationship is of this stratigraphy is critical for oil and gas exploration. Following the advent of horizontal drilling and hydraulic fracturing technology, Granite Wash reservoirs have become an important target for oil and gas exploration. Previous geological studies in the area (Bouma, 2000; Parks 2011) agree

generally in delineating the fan complex into proximal, medial and distal fans. However, geophysically the granite wash formation remains a challenging unit for seismic characterization, especially within areas proximal to the source (Valerio, 2006). Due to rapid change in lithofacies, thickness and bed discontinuities, the identification of specific alluvial depositional environments and reservoir facies from seismic data is not well-documented. The formation consists of five distinct series: The Virgilian, Missourian, Desmoinesian and the Atokan. In this study I focus on characterization of chaotic features and alluvial fans deposited on the Cherokee group of Wheeler and Hemphill counties of the Texas Panhandle with an aim to delineate the granite wash reservoir geomorphology and depositional environment. As part of the overarching objective of this thesis, I applied state-of-the-art seismic processing and data conditioning techniques on the 3D seismic volume acquired over the study area. Due to the complex depositional nature of this play, the seismic data are highly contaminated by coherent and random noise, such as ground-roll, reverberation and air-blast events, resulting in the seismic processing challenge. To improve seismic interpretation, I reprocessed the raw field gathers through, coherent noise suppression, prestack Kirchhoff migration (Verma 2015; Guo, 2014), and other corresponding sophisticated data conditioning techniques.

Chapter 2 of this thesis describes the geological setting of the study area. All of these includes robust information on the tectonic influence, stratigraphic and structural make-up as well as the environment of deposition. Chapter 3 summarizes details of both classic and more recent geoscientific probing in the study area with emphasis on lithologic compositions, depositional environments, data and the methodologies used. Next, I discuss

my seismic reprocessing workflows in Chapter 4, including the survey geometry, linear suppression workflow, prestack time migration, structure-oriented filtering, and finally comparing the reprocessed seismic product to the original products obtained from the vendor.

In Chapter 5, I evaluate multiattribute facies expressions over the entire stratigraphic extent of the Granite Wash formation in an attempt to identify specific alluvial fan depositional patterns and map productive lithofacies while the primary goal is to better understand reservoir heterogeneities.

Here, I generated a suite of select attributes (geometric, textural and poststack inversion attributes that favor seismic geomorphological objectives within a fan depositional context then feed them into an unsupervised clustering algorithm – The Generative Topographic algorithm for facies delineation.

Chapter 2: Geologic Setting

The Anadarko Basin of the Mid-continent is a sedimentary basin within the North American Craton and is considered one of the most productive hydrocarbon basins in the United States (Dutton, 1984; Perry 1989) (Figures 1, 2 and 3). Locally, the Anadarko basin retains the pedigree for the deepest interior basin in North America dominated by more than 40,000 ft. deep Cambrian-Permian sediments, mostly deposited in deep-to-shallow marine environments (Mitchell 2011, Perry, 1989). Perry (1989) divides the structural history of the Anadarko Basin into four stages: (1) The Precambrian crustal consolidation, (2) Late Precambrian to Middle Cambrian to Middle Cambrian southern Oklahoma Aulacogen evolution where large amounts of igneous intrusion and extrusion developed along the axis of the Aulacogen (Gilbert, 1992), (3) the Cambrian through Early Mississippian southern Oklahoma trough creation where the region subsided resulting in a depocenter for carbonates, sandstones and shales (Gilbert, 1992; Johnson, 1989), (4) The Late Paleozoic tectonism resulting from the development of the Amarillo-Wichita uplift.

Deposition of Granite Wash sediments started in this late Paleozoic stage and was accompanied by a change of stress regime from extensional to compressional due to the collision of North America with Gondwana. The deeper portion of the basin lies successively on a basement of faulted Cambrian igneous rocks, which became an upthrust block in this new compressive regime thereby, leading to an increase in the subsidence rate of the Basin (Gilbert, 1992). Extensive episodic uplift occurring during the Early Pennsylvanian through the Permian resulted in the formation of the Amarillo Mountains (Mitchell, 2011; Perry, 1989; Sahl, 1980). Figure (2) shows the Pennsylvanian (Middle) paleogeographic map showing relative locations of the Anadarko Basin, Amarillo-Wichita

Uplift, and the study area (Blakey, 2013; Figure 2). The Granite Wash was deposited during the Pennsylvanian Era due to the dynamic tectonic activity known as the Amarillo Uplift (Mitchell, 2011). Sediment movements from the Amarillo Wichita uplift were deposited in the Anadarko Basin as alluvial fans, debris flows, fan deltas and turbidite flows between the Pennsylvanian Morrowan and Permian Wolfcampian times thus forming the Granite Wash (Mitchell, 2011; Henry and Hester, 1995, Dutton, 1984; Gelphman, 1960). These deposits are a mix of conglomerates, sandstones, and mudstones sourced from the adjacent Amarillo-Wichita uplift with lithologic constituents ranging from chert, dolomite, limestone, gabbro, granite, and rhyolite. The deposits were laid down by a sequence of alluvial fans and fan deltas. Evaporites, deposited in the Permian Era, make up the top seal of the Granite Wash. This energetic depositional environment has led to a variety of rock attributes over short distances in some areas (Ingram, 2006).

The Granite Wash is made up of layers of clastic sediments that are coarse-grained with marine shales and carbonates in between. The porosities range from less than 1% to over 8% and the permeabilities range from 0.0005 mD to 0.285 mD (Rothkopf, 2011). These alluvial fans and fan deltas that make up the Granite Wash are good potential reservoir facies. However, fine-grained layers, cemented faults, or other sealing facies are needed to form a trap. For this reason high lateral and vertical seismic resolution is important in identifying these sealing facies (Dutton, 1982).

Horizontal drilling is ideal to exploit such a reservoir, but the well needs to be kept inside the layer of interest. Layers in the Granite Wash formation can have lateral heterogeneity of less than 3 ft. This occurred because of the natural deposition of sediment and the large

amount of drilling done in the formation. With such a small window, wellbore placement becomes very sensitive to lateral changes (Michell, 2011). With lateral heterogeneity and the changing geology, higher resolution seismic data are necessary if wells are to be drilled economically. Figure 3 and 4 show the structural cross-sections and the stratigraphic column of the Anadarko basin.

The Granite Wash is divided into five main series (Figure 4), namely: Morrowan, Atokan, Desmoinesian, Missourian, and Virgilian. Situated in the lower Pennsylvanian, the Morrowan series consists predominantly of shales with discontinuous sandstones and limestones, hydrocarbon-producing sediments. The Atokan series is represented by a thick wedge of arkosic sandstone and conglomerates adjacent to the uplift and thins towards the northeast. The Desmoinesian series is subdivided into the Cherokee group and the Marmaton group and consists of interbedded arkosic sandstones and conglomerates that thins into shaley units of the northeastern portion of the uplift (Mitchell, 2011). The Missourian and Virgilian series consist of carbonate sediments (especially in the shelf areas) and are predominantly sourced from the Ouachita Mountains and the Amarillo-Wichita uplift (Mitchell, 2011).

This study focuses on the Cherokee-Desmoinesian series of the Wheeler and Hemphill counties, Texas and uses stratigraphic terminologies proposed by Mitchell (2011) in the eastern Texas Panhandle area of the Anadarko Basin. The area is filled with proximal to distal submarine fans expressed as arkosic sandstones and mudstones due to the presence of intrusive rocks caused by the Amarillo-Wichita uplift (Figure 5). These intervals are

separated by distinct radioactive shales in the area that are easily mapped on gamma ray log (Mitchell, 2011). These mudstones are then used as constructs for defining specific stratigraphic zones of interest. Often times, there seems to be an obfuscation about the nomenclature of these Granite Wash intervals with researchers resorting to different stratigraphic terminologies.

Mitchell divided the Desmoinesian Granite Wash intervals of the Marmaton Group into nine zones: Marmaton Wash, Marmaton A to F, for the Cherokee Group into Upper Skinner and Lower Skinner Wash. LoCricchio (2012) defined eleven zones of same interval as Top Marmaton Wash, Britt, and GRWB to GRWJ. Senoglu (2017) interpreted ten stratigraphic zones by using laterally extensive and correlative mudstones as leads for defining these intervals: Marmaton, Caldwell, Cherokee, Granite Wash A (GRWA), Granite Wash B (GRWB). Granite Wash C (GRWC). Granite Wash D (GRWD). Granite Wash E (GRWE). Granite Wash F (GRWF) and Granite Wash G (GRWA).

Figure 4 shows how the stratigraphic nomenclatures and zonation correspond to each other from Senoglu, (2017).

Chapter 3: Previous Work

An enigma of sorts, the lithological and structural history of the Granite Wash remain complex at best. Most of the literature work up till now in the Granite Wash continue to focus broadly on understanding the region's depositional environments their ensuing provenance as well as the lithological and reservoir potential. In this section, I summarize both recent and classic interpretation of the Granite Wash, emphasizing on both the geological and geophysical components. Although, there seems a horde of references on the Wash's geological history but fewer attempts have been made to investigate its geophysical significance.

The Desmoinesian Granite Wash deposits of Wheeler and Hemphill counties, Texas occur as several thousands of feet of conglomerates, sandstones, and shales forming rare a combination of reservoir properties. In the classic works of Sahl (1970), Dutton (1985) and Mitchell (2012), basinward sandstones and mudstones of the Granite Wash were interpreted as medial to distal turbidite and debris flows. These authors also interpreted the depositional environments in the Texas Panhandle and Oklahoma as alluvial fans, deltaic fans and turbidite flows. Uplift forces in the area cause the alluvial fans to be shed as large amounts of weathered rocks which are deposited close to the Amarillo-Wichita uplift thereby creating varying grain sizes and poorly sorted deposits. McGowen (1971) created depositional models by studying modern alluvial fans and fan deltas. McGowen argued that fan deltas and alluvial fans are formed by the same processes but as water levels rises, fan deltas prograde into marine environments.

Using a suite of well logs and core samples to provide descriptions for the lithology and reservoir properties of the Granite Wash intervals, Dutton (1985) investigated the Mobeetie

fields, Wheeler County, Texas-Oklahoma Panhandle and found the area to be a part of a larger fan delta system. Duggins (2013) also studied the facies architecture and the sequence stratigraphy of the Oklahoma-Texas Panhandle but focused more inherently on the Marmaton group. Results from a combination of wireline logs, core samples, spectral gamma ray, and magnetic susceptibility data interpreted the depositional environment of the study area as a fan-delta system. Holmes (2015) also investigated the facies and stratigraphic characteristics of deep water deposits at Colony Granite Wash field, Anadarko Basin. Integrating variations of geological and geophysical data consisting of well logs, cores, X-ray diffraction measurements, and seismic data, Holmes (2015) created three-dimensional models of the architectural elements while using artificial neural networks and a combination of geostatistical measures for lithologic predictions. He also found the area to exhibit features associated with a marine depositional environment including conglomerates, sandstones and mudstones expressed as channels, levees, and upward-fining turbiditic geometries. Salantur (2016) also probed the lithological, stratigraphic and reservoir characteristics of the Marmaton Group, Elk City Field, Anadarko Basin, Oklahoma. He used artificial neural network for lithologic predictions while the sequential-indicator simulation approach was used to map the spatial lithologic distribution and connectivity of the reservoir. Using well-log and core samples, the environment of deposition was interpreted to be a fan delta expressed as conglomerates and sandstones.

Karis (2015) also studied the Marmaton Group in Beckham and Wheeler counties Oklahoma-Texas Panhandle with the aim to investigate the lithologic, stratigraphic and reservoir characteristics of the study area. Wireline logs and cored wells were used to predict key lithologies with the aid of principal component and clustering analysis estimate

to lithologies in non-cored wells. Sequential-indicator simulation was used to map the spatial lithologic distribution while Sequential Gaussian simulation was employed for petrophysical property estimations. The study area was interpreted as terrestrial to shallow marine represented as conglomerates, sandstones and mudstones.

Stratigraphically, Granite Wash intervals are marked by distinct shale breaks which represent regional flooding surfaces (Holmes 2015; Karis, 2015; LoCricchio, 2012). Following this, LoCricchio (2012) defined eleven stratigraphic zones while studying Desmoinesian Granite Wash deposits. Mitchell (2012) also divided the Marmaton Group into seven zones with the Cherokee Group having five distinct zonal divisions; the Upper Skinner Shale, Upper Skinner Wash, Lower Skinner Shale, Lower Skinner Wash and Redfork. In a bid to understand the geomorphology and reservoir characteristics of the Desmoinesian Granite Wash intervals in Wheeler county, Texas, Gavidia (2012) utilized 3D seismic attributes, post stack inversion products and well logs to define nine seismic horizons – Caldwell, Cherokee, and Granite Wash A to G. Using acoustic impedance volumes to map reservoir heterogeneity, sandstones were found to have relatively higher impedance values which is typical of reservoir in the study area. Batista (2010) also generated a suite of geometric and structural attributes to delineate Granite Wash deposits while using acoustic impedance as constrain for evaluating reservoir heterogeneity.

Chapter 4: Seismic Processing and Data Conditioning

Many exploration and production efforts are taking place in complex geologic settings with poor signal-to-noise ratio seismic data, thus making it difficult to find and produce hydrocarbons.

The integrity and reliability of the seismic interpretation for structure, lithology and reservoir characterization are directly related to the signal-to-noise ratio of the seismic data. Consequently, the need for good quality seismic data is of great importance. Attribute Assisted Seismic Processing and Interpretation Group at the University of Oklahoma received seismic data acquired over the Hemphill and Wheeler Counties of the Texas Pandhandle, Anadarko Basin in 2012.

While overall good quality, the seismic data was processed by a third-party processing company but still suffers poorly from residual ground-roll, migration aliasing and relatively low vertical resolution events especially in the shallower sections. It unclear whether these limitations are due to the processing workflow applied by the vendor or to the complex depositional nature of the Granite Wash which affects seismic resolution (Mitchell, 2012). The overarching objective of this chapter is to suppress coherent noise events while preserving frequency content and geologic heterogeneity. In this section, I provide details of the linear noise suppression and seismic data conditioning with the aim to improve the seismic resolution whilst preserving data fidelity.

In 2011, Devon Energy Corporation via a commercial seismic acquisition and processing vendor conducted a seismic acquisition program over a 28-sq. mile area of the Wheeler and Hemphill Counties of the Texas Panhandle, Anadarko Basin. The vendor-processed product includes both 3D wide-azimuth unmigrated and OVT-migrated prestack seismic

volumes. Figure 1 shows the relative location of the survey within the two county areal boundaries while Table 1 shows an outline of the more important acquisition parameters. I have also summarized the vendor-processed prestack gathers sequence in Table 1. My reprocessing sequence are organized into the following tasks:

- Geometry definition
- Linear noise suppression
- Prestack time migration
- Spectral Balancing
- Poststack structure-oriented filtering
- Comparison of reprocessed data to data provided by the commercial service processing shop.

Figure 6 show my generalized processing workflow as well as the graphical breakdown of the linear noise suppression procedures.

1. Data loading and geometry definition

Usually the first step of any seismic processing endeavor, loading seismic data into the processing software is arguably the most important step of a sequence of processing objectives as it requires inputs of key acquisition parameters (Table 1) as well as header byte locations (Table 2), which, when not available or improperly utilized may stall or affect later processing steps. Fortunately, this information was stored in the EBCIDIC header of the seismic dataset were applied accordingly. Figure 7 show the source and receiver geometry with sources locations represented as red square boxes trending in the East-West direction. Receiver locations (North-South) are represented as deep blue circles,

trending the North-South direction. Figure 8 also shows common shot gather spatial geometry. The active receivers corresponding to the shot are represented as yellow circles. Figure 8 shows a representative common shot gather with active (or "live'') receivers in yellow corresponding to the source in green.

In this example, the active receivers fall along 17 receiver lines, defining a "patch''. Several of these receiver lines forming the patch are displayed in Figure 9 where the ground roll travelling ''broadside'' to a receiver line exhibits hyperbolic moveout (in orange). This hyperbolic moveout is similar to that of reflection events of interest. Figure 10 shows the entire shot gather sorted by source-receiver offset where the trace-to-trace separation is now irregular. Note the near linear moveout of ground roll and reverberations when the gather is deployed in this manner. However, adjacent traces in this sorted gather are not necessarily adjacent in (x, y) space making filtering difficult.

After loading the data and quality controlling the geometry, the next step is to define a binning layout. The natural bin size used for this survey was set to 110 ft x 110 ft since the inline source and receiver intervals are both 220 ft respectively. After binning, I generated the fold map the survey shown in Figure 11. The survey has a maximum fold of 250 and a mean fold of 125 traces per bin.

2. Linear noise suppression (LNS)

The linear noise suppression workflow presented in this thesis (Figure 6) followed those of Ha (2015) and Verma's (2015) applied to different Paleozoic targets in Texas. For this reason, I have skipped the details of the technique. Since the data was pre-processed by a vendor company, some preliminary processing steps (Table 4) have been applied prior to

implementing the LNS. According to the processing report, coherent and surface consistent noise suppression methods were applied. Nevertheless, specific intervals, especially seismic signals in the shallow sections down to the target formation (Cherokee formation, t =~ 1.8s – 2.06s) still suffer severe ground roll contamination (Figures 9 and 10). The linear noise suppression technique was applied to eliminate the residual ground roll events, increase the signal-to-noise ratio while preserving signal integrity for subsequent velocity analysis and migration results. The general principle of the linear suppression workflow is provided below (in chronological order):

a.) Noise Isolation by muting and band-pass filtering to remove high frequency signal.

b.) Noise flattening using a linear moveout (LMO) velocity

c.) Modeling the noise

d.) Unflattening the modeled noise by inverse LMO

e.) Subtracting the modeled noise from the original data

Figure 12 shows the original common midpoint gather before the linear noise suppression. The blue arrows in the figure indicate areas contaminated by the ground roll events. The workflow begins with band-pass filtering and windowing the ground roll contaminated zone. This way, subsequent filters will not influence reflection events outside the windowed ground roll zone. Then, linear moveout corrections were applied using the average phase velocity of the ground roll, thereby obtaining a relatively flattened ground roll event. This process created a patched version of the data thus making it amenable to 3-D edge preserving structured-oriented filtering (Marfurt, 2016). After this, residual inline and crossline components as well as coherence were

computed within an analysis window to account for variations in velocity, thickness and weathering topography. Using a Kuwahara algorithm, the most coherent window that best represents moderately dipping coherent ground roll event is subjected to a structured-oriented Karhunen Loeve (KL) filter to model the coherent ground roll noise. The criteria for choosing the window is such that, if a window is satisfactorily coherent, the Karhunen Loeve (KL) filter is applied to model the moveout-corrected event. On the other hand, if the window is incoherent (misaligned random noise or signal) the filter is not applied. Finally, the linear moveout effect is removed from the modeled ground roll and subtracted from the original data. The final common midpoint gather after the linear suppression implementation is shown in Figure 13.

Figure 14 also shows the common mid-point gather showing the difference between the gathers before and after the implementation of the linear noise suppression workflow. This difference represents the isolated ground roll noise which is subsequently modeled and subtracted from the original data. Shot gathers sorted by shot vs. channel numbers of the original, final and isolated noise (difference) are also shown in Figures 15, 16 and 17 respectively.

3. Prestack Time Migration

Seismic migration relocates dipping events to their correct subsurface locations while creating a more accurate image of the subsurface. Following the successful implementation of the linear suppression workflow, the data was passed for subsequent Prestack time migration with the aim to fix possible issues associated with the acquisition. The prestack gather was migrated using a Kirchoff prestack time migration (PSTM) algorithm described

by Perez and Marfurt (2008) using the velocity volume computed from unmigrated CMP velocity scans. Figure 18 shows the results after migration (left) before and (right) after muting to remove the stretched reflectors at far offsets. Figure 18 shows the resulting stack section after the stretched offsets were muted. The image shown here focuses on areas around the target interval of interest to emphasize on ensuing improvements introduced by the processing workflow.

4. Data Conditioning

The process of post-stack data conditioning seeks to eliminate possible cross-cutting high and low frequency noise/migration artifacts which may have been sourced from migration aliasing artifacts introduced by the Kirchoff prestack time migration. After the prestack time migration, the resulting volume was stacked as shown in Figure 19. Notice the appearance of some steeply dipping cross-cutting noise on the data suspected to have been introduced by migration process. To suppress this noise/artifacts, I applied Continuous Wavelet Transform (CWT) spectral balancing as well as 3-iterative processes of structured-oriented filtering algorithms to the stacked data. The details of the workflow are discussed in the subsequent sections.

5. Spectral Balancing

To improve the frequency content of the seismic stacked data, especially with regards to improving low temporal frequencies appearances caused by possible wavelet rotations at the lateral edges of the migration operator which is caused by very low vertical

wavenumber in the time migration domain, Chopra and Marfurt's (2016) CWT amplitude-friendly spectral balancing method was implemented.

The algorithm is implemented by first decomposing the data into time-frequency spectral components, then, the power of the spectral magnitude (PSM) is computed for each sample and frequency window and then averaged over all the entire traces in the spatial volume. This average power spectrum is further smoothed within a 500 milliseconds running window at each sample. The peak of this average power spectrum is computed and used alongside the average power spectrum to design a single time-varying spectral operator. The results of the methods application to stacked data is shown in Figures 20 and 21. Figure 20 shows the unbalanced poststack seismic volume. Notice the appearance of some steeply dipping cross-cutting noise on the data as well as the time variant frequency distribution on the right. Figure 21 show an improved output after the spectrally balancing where the low apparent frequency cross-cutting noise is suppressed. The frequency spectrum of the data after the spectrally-balanced data now shows a broader band response when compared to the frequency content of the original unbalanced input data.

6. Structured-Oriented Filtering (SOF)

To further improve the quality of the spectral-balanced volume, I applied the poststack structured-oriented filter with the aim to enhance reflector continuities while preserving geologically-reasonable features. The SOF algorithm bases its principle on the theoretical formulation of Hoeckers and Fehmers (2002) on anisotropic diffusion as well as the early works of Luo et al. (2002) on Kuwahara filtering. Inputs to the SOF program include the spectrally-balanced seismic amplitude volume, inline and crossline dip components as well as similarity attribute measures of the seismic volume. The output generated by this

program come in different filtered versions, the principal component or Karhunen-Loéve, mean, median, and alpha-trimmed-mean volumes. However, the PC-filtered displayed the best results of these five options. Although, not as computationally-demanding as the migration process, the SOF would usually require a number of iterations, in this case, three iterations, to produce the desired results. Figure 22 shows the result obtained after the third SOF iteration. The image shows an improved version of pre-conditioned volume. A display of the rejected noise after the implementation of the structured-oriented filter is shown in figure 23.

7. Comparison of reprocessed data to data provided by the commercial service processing shop

In this section, I compare the original (vendor-processed) poststack time migrated data to the reprocessed stacked data to quality control my processing workflow. Figure 24 shows side-by-side vertical slices through the original and reprocessed data. As seen on the image, the reflectors on the reprocessed data exhibit broader bandwidth and are more continuous. Arrows indicate major improvements on the data. Figure 25 shows time slices through the original (vendor) and reprocessed data at t = 1.8s (near the target formation). Here, the amplitudes are more continuous (yellow arrows) and the footprint suppressed. The footprint suppression is more pronounced on coherence attribute (Figure 26) time-slice extracted at t = 1.9s.

Advances in processing methods such as the linear suppression workflow proposed by Verma et al., (2015) and the application of structured-oriented filtering for suppressing incoherent noise both contribute to the quality of the reprocessed data.

Chapter 5: Seismic Interpretation and Facies Analysis

In this chapter, I summarize the details of my stratigraphic interpretations as well as the process of my poststack inversion efforts. Following this, I also evaluate multiattribute facies expressions over the entire stratigraphic extent of the Granite Wash formation in an attempt to identify specific alluvial fan depositional patterns and map productive lithofacies. I generated a suite of geometric, textural and poststack inversion attributes that favor seismic geomorphological objectives within a fan depositional context. I then feed them into an unsupervised generative topographic mapping algorithm for facies delineation. These investigations are limited to the Cherokee intervals of the Wash due to their excellent petrophysical responses and also the availability of completed horizontal wells within the units (Gavidia, 2002).

Structural and Stratigraphic interpretations

To identify the key horizons in the reprocessed seismic data, synthetic seismograms were generated and tied to Wells A, B, C and D in the survey. This process helps to correlate information obtained from well-logs (lithology) to the seismic reflector responses. Using these ties, it is possible to identify key stratigraphic horizons across the Buffalo survey. Next, I interpreted nine major horizons within the Desmoinesian-Pennsylvanian extents. These are: Granite Wash Caldwell, Granite Wash Cherokee and Granite Wash A through G. Figure 27 shows a vertical section through A-A' showing key Granite Wash horizons. I interpret up-dip thinning packages towards the west as an evidence of syndepositional tectonics. The dashed line also shows the major fault in the survey.

The Cherokee occurs at approximately at t = 1.8s. Figure 28 shows the time structure map of the Cherokee and the GRWG formations. Figure 29 also shows the time-thickness map of the Cherokee-GRWG interval of the Granite Wash. I interpret sediments deposition to the south, where sediments are thickest, to be potential alluvial fans movements that thins as the fans prograde towards the deeper portion of the basin.

Seismic Facies Analysis

Although considered one of the most productive oil and gas reservoir in the United States (Mitchell, 2011), the Pennsylvanian-age Granite Wash reservoir remain an enigma of sort. Amongst a myriad of issues that currently plagues its existence are an unusually low porosity and permeability estimates, varying grain sizes, mineralogy, cementation and presence of micro-fractures. These have not only influenced its complex stratigraphic and structural depositional pattern but have also made the formation difficult to image seismically. To better understand the reservoir geomorphology and lithological heterogeneity, I generate what may be the first seismic facies analysis of the Desmoinesian-Cherokee wash of Wheeler and Hemphill counties, Texas using seismic attributes (geometric and textural) and inversion technique to map specific alluvial fan depositional environments and reservoir facies from seismic data as well identifying productive chaotic facies using these attributes. I will use an unsupervised latent space modeling technique: The Generative Topographic Mapping (GTM) algorithm to classify rock-facies types and reservoir quality using well log as ground truth.

Seismic Attributes Selection

My choice of attributes is guided by the objective to differentiate alluvial fan from more chaotic facies. Roy et al., (2014) used multiattribute facies analysis to map both lateral and vertical lithofacies heterogeneities in a complex carbonate wash in the Vera Cruz basin, Mexico. In my case, I will use coherence, coherent energy, curvature, peak frequency, GLCM entropy, GLCM homogeneity, P-impedance and reflector convergence to map a granite wash. Coherence measures waveform similarities and enhances our ability to visualize structural and stratigraphic discontinuities on horizon slices. Figure 30 shows a coherence time slice extracted along the Cherokee wash. In this figure, the fan edges are pronounced and easy to delineate. Figure 31 also shows co-rendered coherence and coherence energy attributes where we see a relatively higher coherent energy response in certain portions on the time-slice bounded by the fan geometry.

Figure 32 shows a gray-level co-occurrence matrix (GLCM) entropy texture attribute. This attribute provides measures of disorderliness or complexity of a seismic image and thus quantifies the lateral variations of reflectivity along structural presence. P-impedance is a more direct measure of lithology and fluid content. Four wells (Wells A, B, C, D) in my survey have P-sonic and density logs, allowing me to invert for P-impedance. However, because there are no shear-sonic logs in this survey, I could not conduct prestack inversion. To validate the efficacy of my processing effort, I compare results of the well-seismic tie procedures using the vendor-processed data and the reprocessed data for Wells A and D. As expected, the correlation obtained on the reprocessed data was higher than obtained for the vendor data. Figures 33, 34, 35 and 36 show these comparisons for Wells A and D.

Figure 35 shows the acoustic impedance extracted along the Cherokee horizon. Dry Well C corresponds to a relatively high impedance value while Oil and Gas producing well E corresponds to relatively low impedance values. This result is corroborated with Senoglu's (2017) well logs crossplot of acoustic impedance versus porosity (Figure 36).

Figure 37 also shows co-rendered most-negative curvature and P-impedance volume. Here, relatively low AI values correspond to 'valley' estimates of the curvature anomalies. Reflector convergence structural attributes (not shown) also map whether reflectors are conformal or pinching out (Chopra et al., 2008)

GTM

I apply generative topological mapping classification technique (Wallet et al., 2009) to the eight seismic attributes discussed above. As the name implies, this non-linear projection technique provides a probabilistic representation of the data vectors in a corresponding lower dimensional space.

In our implementation at OU (Roy, 2014), GTM fits a two dimensional surface to the eight-dimensional data using a probability density function. The algorithm starts with an array of grid points projected onto a two dimensional plane defined by the first two eigenvectors. Respective grid points are then mapped in a non-linear pattern onto a similar dimensional non-Euclidean curved surface as vector ($\mathbf{m_k}$) projected into a different dimensional space in GTM. Respective data vectors ($\mathbf{x_k}$) mapped to this space are then modeled as a group of Gaussian PDFs centred on these reference vectors ($\mathbf{m_k}$).

I applied the GTM algorithm to our select attributes using coherence, coherent energy, peak frequency, reflector convergence, GLCM entropy and heterogeneity and P-impedance attribute volumes and derived GTM 1 and GTM 2 outputs. These attributes then result in

cluster locations along the two axes in the latent space to be utilized when cross-plotting (Figure 37). Figure (39) shows same time-slice extract along the Cherokee wash through cross-plotting GTM-1 and GTM-2 projections. The pink color delineations are interpreted as Facies 1 (pink), Facies 2 (dark green) and Facies 3(lemon green). It is observed that Well C (Dry well) prongs through the pink-colored lithofacies.

To infer the facies-types by the GTM unsupervised predictions, I use lithology estimates obtained from Senoglu (2017) to validate my result. In her work, she used facies descriptions from two cored samples to derive lithology predictions for non-cored wells in the study area. Using a combined artificial neural network and well-log cutoff with gamma-ray, resistivity and Vshale logs, lithology logs were obtained for Wells A, B, C, D and E with an accuracy of about 84% (Figure 40). Following estimates from the lithofacies predictions, Facies 1 correspond to sandstones while Facies 2 and 3 could be either muddy sandstones or mudstones.

The use of geometric, textural and inversion attributes is demonstrated to be a powerful tool in delineating discrete depositional environments like the Cherokee Wash. Moreover, by combining different geometric attributes with inverted AI it is possible to build geomorphological model and also delineate lithological heterogeneity within the Cherokee wash. The use of multi-attributes also makes it possible to identify fan deposits in the areas.

Chapter 6: Conclusions

The primary goal of this study was to use seismic attributes and facies classifications to map productive facies in the Granite Wash of the Texas-Panhandle and Western Oklahoma. Due to the complex depositional nature of the study area, the seismic data suffers poorly from coherent noise expressed as ground roll and reverberation noise, migration aliasing and relatively low signal-to-noise ratio especially in the shallow sections and the parts of the target zone. For this reason, a secondary goal was to reprocess the seismic data to suppress coherent noise and broaden the frequency content. To eliminate these coherent noise events, I applied a novel linear noise suppression workflow to the data, which involves the process of isolating the contaminated ground roll zone which is subsequently modeled and subtracted from the original data. As hoped, the technique suppressed the residual ground roll events while preserving signal integrity for better velocity analysis and prestack time migration. Subsequent data conditioning process such as the spectral balancing and the structured-oriented filtering procedures were applied thus suppressing crosscutting low frequency noise and enhancing reflector continuities. Compared to the original vendor volume, the re-processed volume, the reflectors, which were not previously visible are now identifiable and expressed broadband continuous reflectors in the reprocessed volume.

To understand the reservoir geomorphology and lithological heterogeneity, I report what I believe is the first seismic facies analysis of the Desmoinesian-Cherokee wash using seismic attributes (geometric and textural) and inversion technique to map specific alluvial fan depositional trend and reservoir geomorphology and heterogeneity from seismic data. Co-rendered coherence and coherent energy attributes provided useful images that

delineate fan geometries from other depositional trends. Acoustic impedance and texture attributes further established correlations between 'productive' facies and chaotic depositional fan-like features. I combined these attributes using an unsupervised Generative Topographic Mapping technique for facies clustering. The result obtained showed three-color clustered facies in the Cherokee interval corresponding to three different facies – Facies 1, 2 and 3. Results from Senoglu's (2017) in the same study area estimating facies-types from cored wells applied to non-cored wells using artificial neural network and gamma-ray cut-offs with an accuracy of 84% were used as constraints to estimate the facie-types through the Cherokee Interval. Following estimates from the lithofacies predictions, Facies 1 correspond to sandstones while Facies 2 and 3 could be either muddy sandstones or mudstones.

References

Batista, A. M., 2010, Evaluation of 3D Seismic attributes and post stack inversion methods: Pennsylvanian Granite Wash reservoir characterization case study, Texas: M.S. thesis, University of Oklahoma, p. 1-8.

Blakey, R., 2013, Paleogeography and geologic evolution of North America, http://cpgeosystems.com/paleomaps.html, (accessed March, 2016).

Bouma, A.H., 2000, Fine-grained, mud-rich turbidite systems: model and comparison with coarse-grained, sand-rich systems, in A.H. Bouma and C.H. Stone, eds., Fine-grained turbidite systems: AAPG Memoir 72/SEPM Special Publication **68**, 9-20.

Cardott, B. J., and M. W. Lambert, 1982, Thermal maturation by vitrinite reflectance of Woodford Shale, Anadarko Basin, Oklahoma: AAPG Bulletin, **69**, 1982–1998.

Chopra, S., and K. J. Marfurt, 2008, Seismic attributes for prospect identification and reservoir characterization: SEG Geophysical Developments Series 11.

Duggins, W. T., 2013, Facies architecture and sequence stratigraphy of part of the Desmoinesian Granite Wash, Texas Panhandle and Western Oklahoma: master's thesis, University of Tulsa.

Durrani, M. Z. A., K. Willson, J. Chen, B. Tapp, and J. Akram, 2014, Rational rock physics for improved velocity prediction and reservoir properties estimation for Granite Wash (tight sands) in Anadarko Basin, Texas: International Journal of Geophysics, 2014, 209351, http://dx.doi.org/10.1155/2014/209351.

Dutton, S. P., 1985, Fan-delta Granite Wash of the Texas Panhandle: Oklahoma City Geological Society Short Course, 1–144.

Dutton, S. P., and L. S. Land, 1985, Meteoric burial diagenesis of Pennsylvanian arkosic sandstones, southwestern Anadarko Basin, Texas: The American Association of Petroleum Geologists Bulletin, **69**, no. 1, 22-38.

Gavidia, G. E., 2012, Attribute supported seismic geomorphology and reservoir characterization of the Granite Wash, Anadarko Basin, Texas: M.S. thesis, Oklahoma State University, Oklahoma City, Oklahoma, p. 1-20.

Gilbert, M. C., 1983, Timing and chemistry of igneous events associated with the Southern Oklahoma aulacogen, in Morgan, P., and Baker, B.H., ed., Processes of continental rifting: Tectonophysics, 94, 439-455.

Gilman, J., 2012, Depositional patterns, source rock analysis identify Granite Wash fairways: The American Oil and Gas Reporter, August 2012 Cover Story.

Guo, S., B. Zhang, S. Verma, and K. J. Marfurt, 2014, Vector correlation of AVAz and curvature attribute – Application to Mississippian Tripolitic Chert, Osage County, Northeast Oklahoma: SEG Expanded Abstract, 346 – 350.

Holmes, C. D., 2015, Stratigraphic architecture, facies characteristics, and distribution of deepwater deposits, Colony Granite Wash, Anadarko Basin, Oklahoma, master's thesis, University of Oklahoma, 166p.

Henry, M. E., and T. C. Hester, 1995, Anadarko Basin Province (058): US Geological Survey National Oil and Gas Assessment, U.S. Geological Survey, Central Energy Resources Team, 47p.

Holmes, C. D., 2015, Stratigraphic architecture, facies characteristics, and distribution of deepwater deposits, Colony Granite Wash, Anadarko Basin, Oklahoma, master's thesis, University of Oklahoma, 1 – 166 p.

Johnson, K. S., and K. V. Luza, 2008, Earth sciences and mineral resources of Oklahoma, Educational Publication 9, Oklahoma Geological Survey, 22 p.

Karis, A. M., 2015, Stratigraphy and reservoir characteristics of the Desmoinesian Granite Wash (Marmaton Group), Southern Anadarko Basin: M.S. Thesis, University of Oklahoma, 1 – 87 p.

Infante-Paez, L., and K. J., Marfurt, 2017, Seismic expression and geomorphology of igneous bodies: A Taranaki Basin, New Zealand, case study, Interpretation, 5(3), SK121-SK140. https://doi.org/10.1190/INT-2016-0244.1

LoCricchio, E., 2012, Granite Wash play overview, Anadarko Basin: Stratigraphic framework and controls on Pennsylvanian Granite Wash production, Anadarko Basin, Texas and Oklahoma, AAPG Annual Convention and Exhibition: Long Beach, California, p. 1-17.

McConnell, D. A., M. J. Goydas, G. N. Smith, and J. P. Chitwood, 1989, Morphology of the frontal fault zone, southwest Oklahoma: Implications for deformation and deposition in the Wichita uplift and Anadarko basin: Geology, **18**, no. 7, 634 – 637p.

McGowen, J., 1971, Alluvial Fans and Fan Deltas: Depositional Models for Some Terrigenous Clastic Wedges, AAPG Bulletin, **55**, no. 1, 125-155.

Mitchell, J., 2011, Horizontal drilling of deep Granite Wash reservoirs, Anadarko Basin, Oklahoma and Texas: Shale Shaker, v. 62, no. 2, p. 118–167.

Mitchell, J., 2015, Economic development of Pennsylvanian age Granite Wash reservoirs with horizontal wells in the Anadarko Basin, AAPG Education Directorate Forum, Granite Wash and Pennsylvanian Sand, Oklahoma City, Oklahoma, 59p.

Olorunsola, O., J. Qi, L., Infante, B., Hutchinson, and K. J., Marfurt, 2016, Multiattribute seismic-facies expressions of a complex granite wash formation: A Buffalo Wallow Field illustration. In SEG Technical Program Expanded Abstracts, pages 1884–1888, https://doi.org/10.1190/segam2016-13946878.1

Perry, W. J., 1989, Tectonic evolution of the Anadarko Basin region, Oklahoma, U.S. Geological Survey Bulletin 1866, 19p.

Roy, A., A. S. Romero-Peláez, T. J. Kwiatkowski, and K.J. Marfurt, 2014, Generative topographic mapping for seismic facies estimation of a carbonate wash, Veracruz Basin, southern Mexico: Interpretation, 2, SA31–SA47, http://dx.doi.org/10.1190/INT-2013-0077.1.

Valerio, C., 2006, Evaluation of spectral inversion and spectral decomposition methods: Pennsylvanian Granite Wash reservoir characterization case study: M.Sc. thesis, University of Oklahoma, 56p.

Verma, S., S. Guo, and K. J. Marfurt, 2015, Prestack suppression of high frequency ground roll using a 3D multiwindow KL filter: Application to a legacy Mississippi Lime survey: SEG Expanded Abstract, 4274-4278p.

Sahl, H. L., 1970, Mobeetie field, Wheeler County, Texas: Shale Shaker, **20**, 107-115p.

Salantur, B., 2016, Continuity, connectivity and reservoir characteristics of Desmoinesian fan-delta conglomerates and sandstones, Elk city field, Anadarko Basin, Oklahoma, M.S. thesis, University of Oklahoma, 53p.

Senoglu, D., 2017, Reservoir Characterization and modeling of the Desmoinesian series Granite Wash, Buffalo Wallow Field, Anadarko Basin, Texas, 65p.

Wallet, B., C., M. C. de Matos, J. T. Kwiatkowski, and Y. Suarez, 2009, Latent space modeling of seismic data: An overview: The Leading Edge, **28**, 1454–1459, http://dx.doi.org/10.1190/1.3272700.

Appendix A: Tables

Table 1: Acquisition properties of prestack seismic dataset

Source type	**Vibroseis**
Trace length	4.8s
Sample interval	0.002s
Vibrator sweep frequency	5-90Hz
Shot Interval	220ft
Shot line interval	220ft
Common Mid-Point bin size	110ft x 110ft
Average Fold	250
Spatial unit (X, Y, Elevation)	feet
Coordinate Reference System (CRS)	Texas North 4201, USA

Table 2: Useful header byte locations of prestack seismic dataset

Header	Byte
FFID (FFID Record Number)	9-12
Channel Number	13-16
Source Station Number	197-200
Source Line Number	193-196
Source X-coordinate	73-76
Source Y-coordinate	73-76
Source Elevation	77-80
Receiver Station Number	45-48
Receiver Line Number	185-188
Receiver X-coordinate	181-184
Receiver Y-coordinate	85-89
Receiver Elevation	41-44

Table 3: Processing history of the prestack seismic data

#Description
Coherent high amplitude noise suppression
Spiking deconvolution
Surface consistent noise correction
Refraction statics
Velocity analysis
Pre-migration scaling

Appendix B: Figures

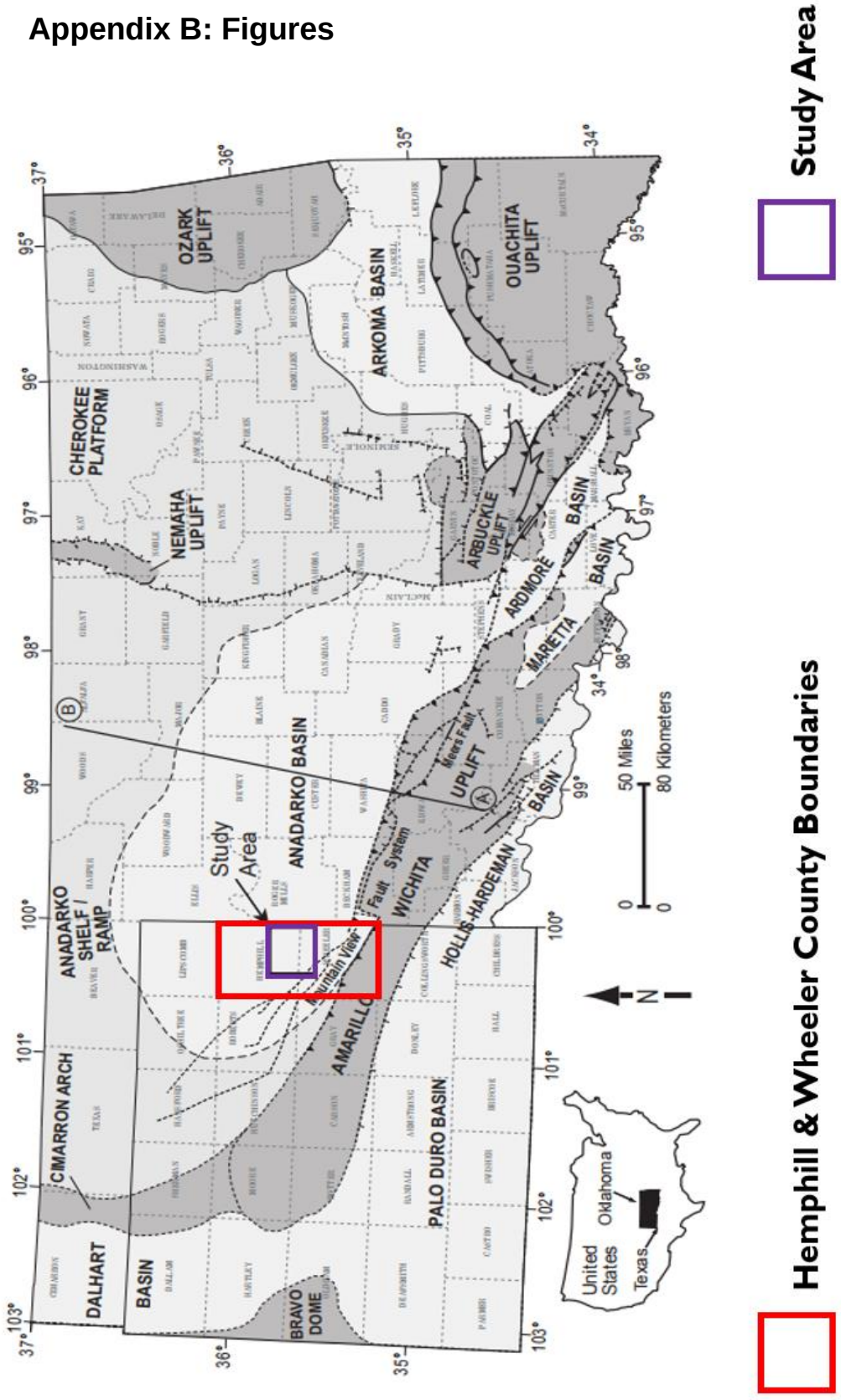

Figure 1: Regional basemap showing key tectonic provinces of Oklahoma and Texas. The red bounded rectangle depicts the Wheeler and Hemphill Counties while the study area (purple rectangle) resides in the deep Anadarko Basin just north of the Amarillo-Wichita Uplift Mountain View Fault System (modified from Johnson and Luza, 2008; Dutton, 1984; McConnell, 1989; LoCriccho, 2012).

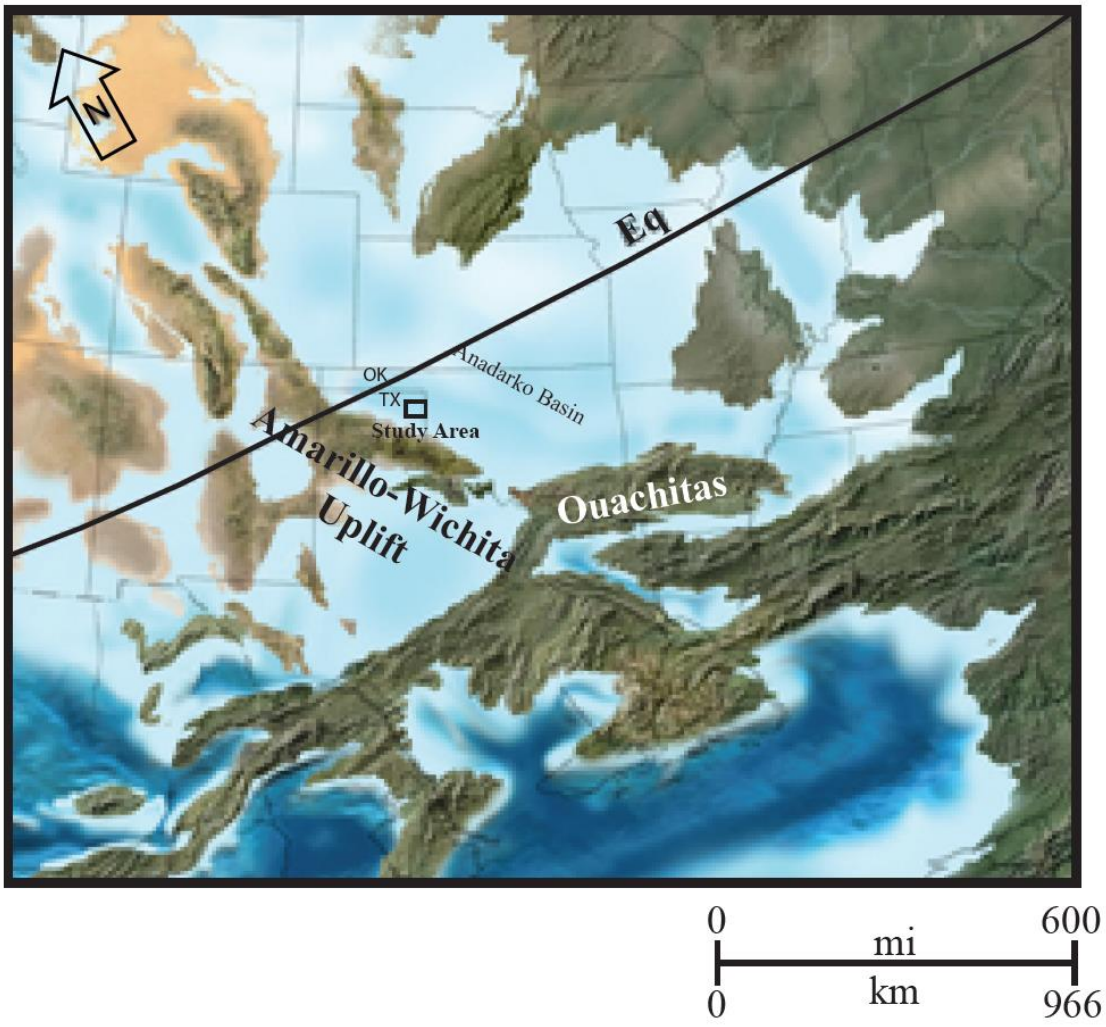

Figure2: Middle Pennsylvanian (308 Ma) paleogeographic map (remodified from Blakely, 2013). Study area is shown in black square. The Amarillo-Wichita uplift was formed during the Early Pennsylvanian at the outset of compressional regime when the Anadarko Basin began to subside. The Amarillo uplift and the study lie relatively south of the Equator.

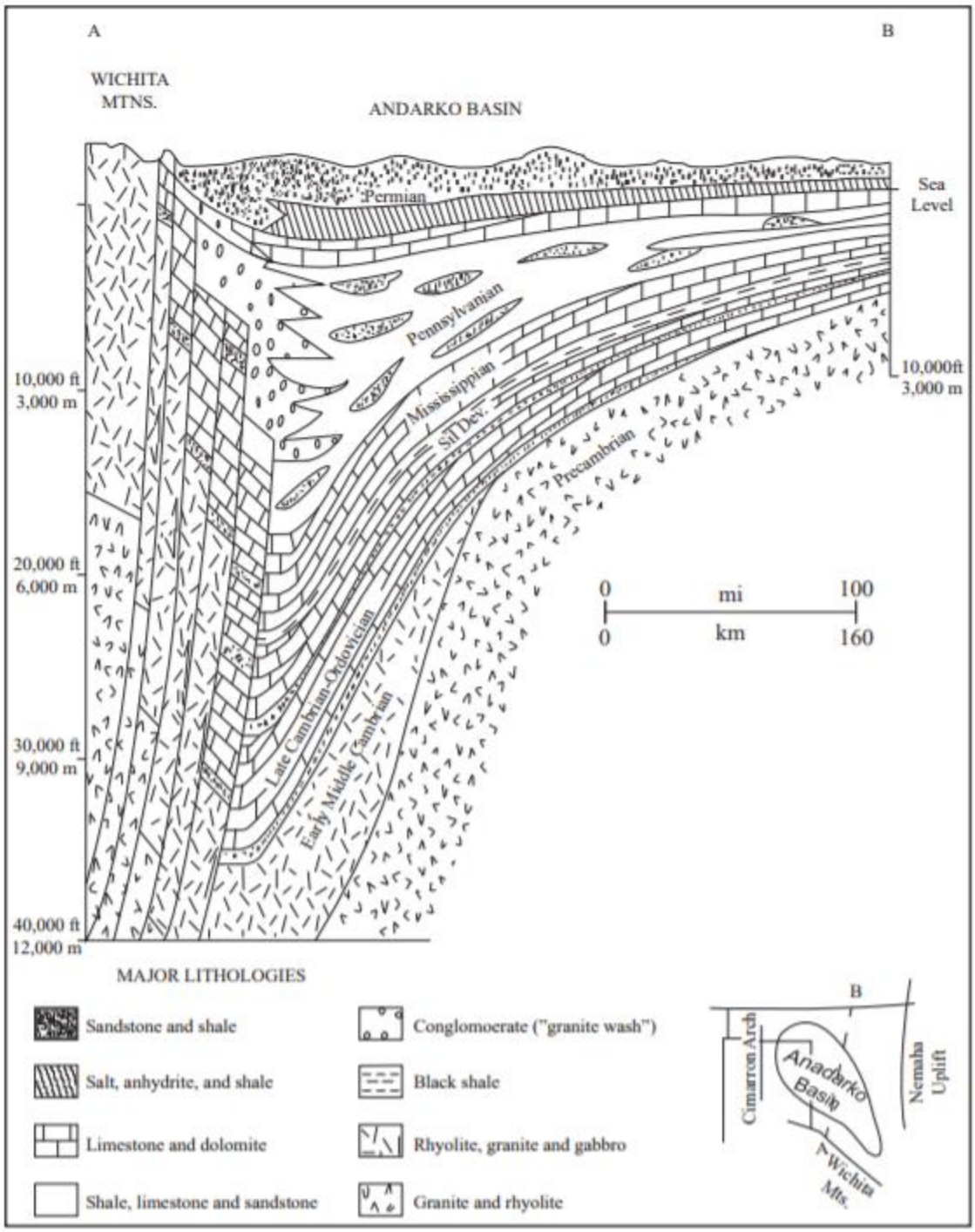

Figure 3: Structural cross-section (SW-NE) of the Anadarko Basin. Following the stress change in the Early Pennsylvanian, the sediments of the Amarillo-Wichita uplift were eroded and deposited in the basin overlying igneous and carbonate rocks. As seen in this diagram, Granite Wash materials pinch out towards north and are transitional with the sediments that are sourced from the north (modified from unpublished by H.G. Davis reported by K.S. Johnson, 1989). The location of this cross-section is seen on Figure 1.

SYSTEM	SERIES	GROUP	UNIT	A	B
PENNSYLVANIAN	VIRGILIAN	Shawnee/Cisco	Shawnee Wash Heebner Sh		
		Douglas/Cisco	Haskell Sh Tonkawa Ss		
	MISSOURIAN	Lansing/Hoxbar	Cottage Grove Wash		
		Kansas City/Hoxbar	Hoxbar Wash/Shale Hogshooter Wash Checkerboard Wash Cleveland Wash		
	DESMOINESIAN	Marmaton (Glover/Big Lime/ Oswego)	Marmaton Wash Caldwell Cherokee GWA GWB GWC	Marmaton Wash Marmaton A Marmaton B Marmaton C Marmaton D Marmaton E Marmaton F	Marmaton Wash Britt GWB GWC GWD GWE GWF
		Cherokee (Skinner/Pink Lime/ Red Fork)	GWD GWE GWF GWG	Upper Skinner Wash Lower Skinner Wash	GWG GWH GWI GWJ
	ATOKAN	Atoka	Atoka Wash 13 Finger Ls		
	MORROWAN	Morrow	Upper Morrow Lower Morrow		

Figure 4: Stratigraphic column and nomenclature of the Granite Wash, Eastern Texas Panhandle, Anadarko Basin. The Desmoinesian Granite Wash has different nomenclature in different states; guide A (modified from Mitchell, 2011) and guide B (modified from LoCricchio, 2012) can be used to correlate Texas and Oklahoma Granite Wash Intervals. Producing interval are represented by the well symbol (Figure modified from Senoglu, 2017).

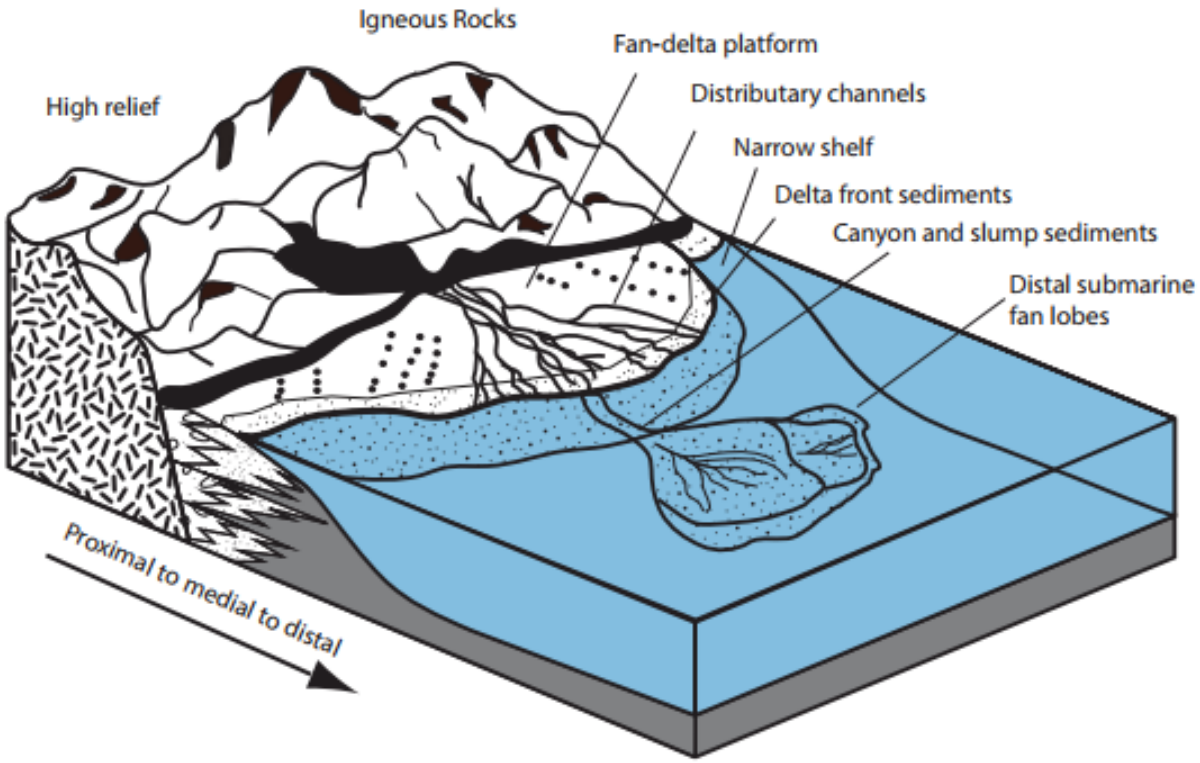

Figure 5: Schematic illustration of the depositional environment of the Granite Wash, Anadarko Basin. Sediments are transported from the Amarillo-Wichita Uplift and are deposited to the mountain fronts as fan deltas. Distal areas are prone to fine-to-coarse grained submarine deposits and are grossly eroded by sediment gravity flows and slumps. Alluvial fan and fan deltaic system are associated with coarse proximal deposits while distal submarine fan lobes consist of finer grain sediments. (Modified from Bouma, 2000; from Salantur, 2016)

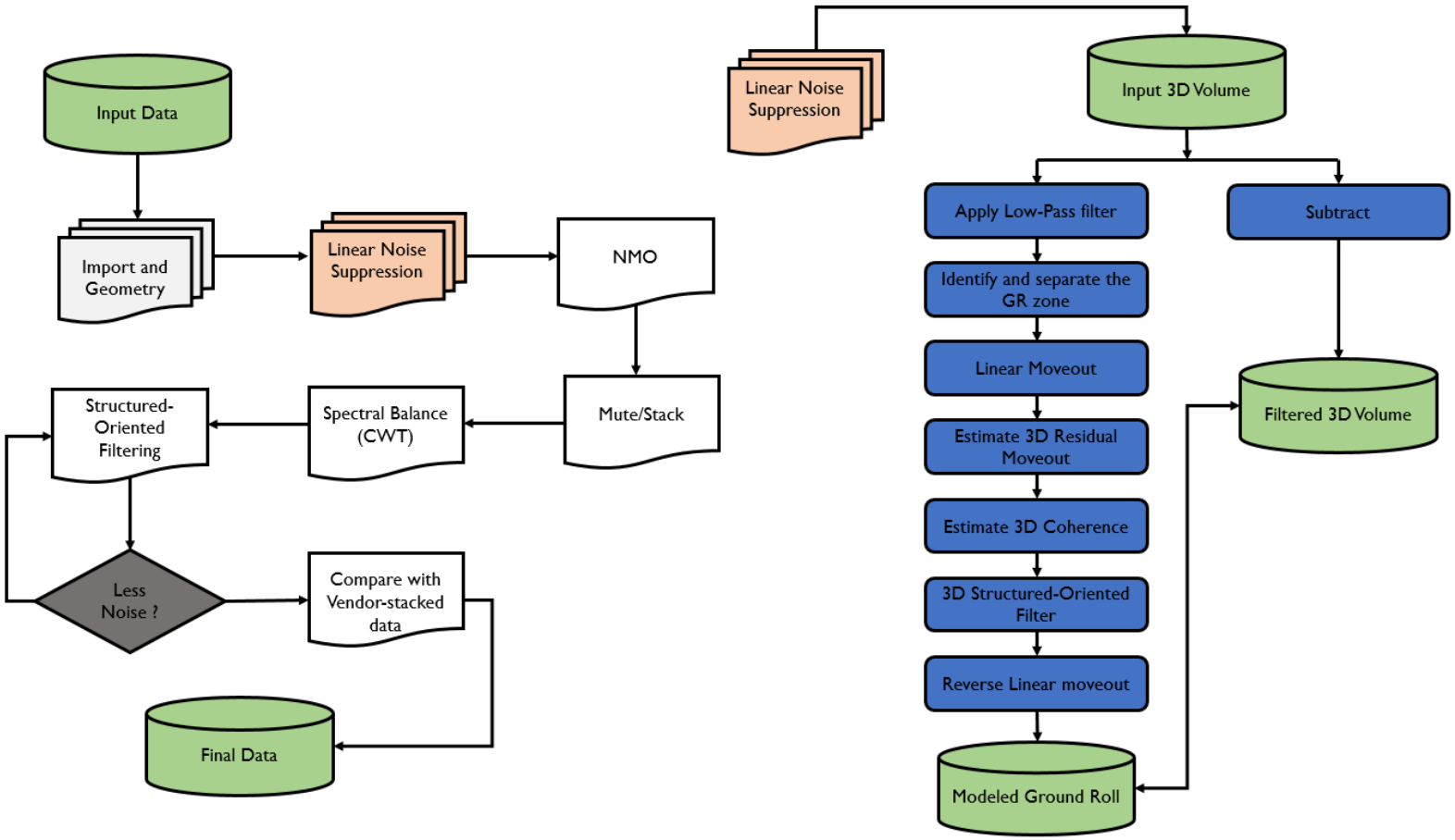

Figure 6: (Left) Generalized seismic processing workflow used in this thesis (right) Seismic linear noise suppression worklflow (modified from Verma et al, 2015)

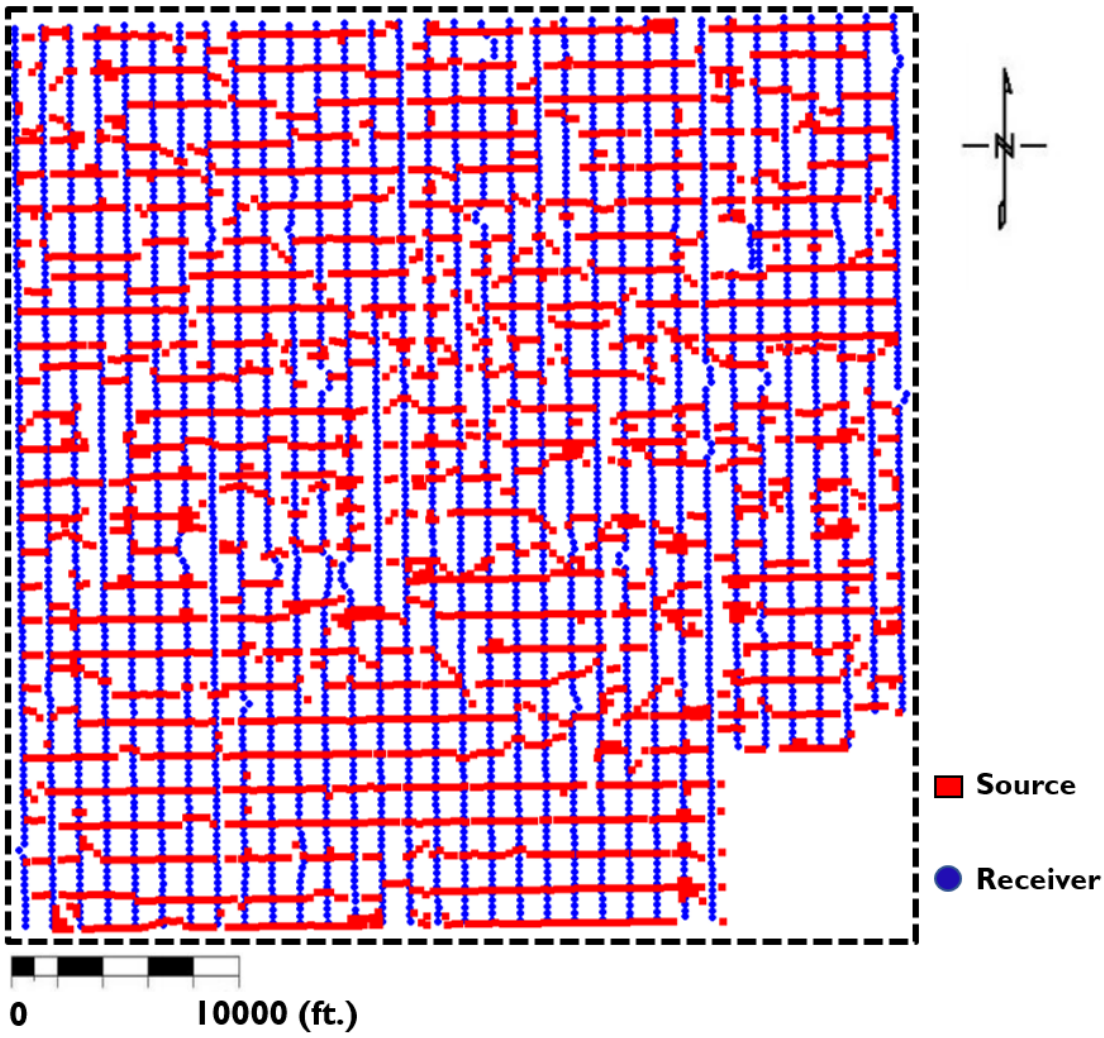

Figure 7: Source and receiver geometry. Red squares represent source locations while blue circle represent receiver locations.

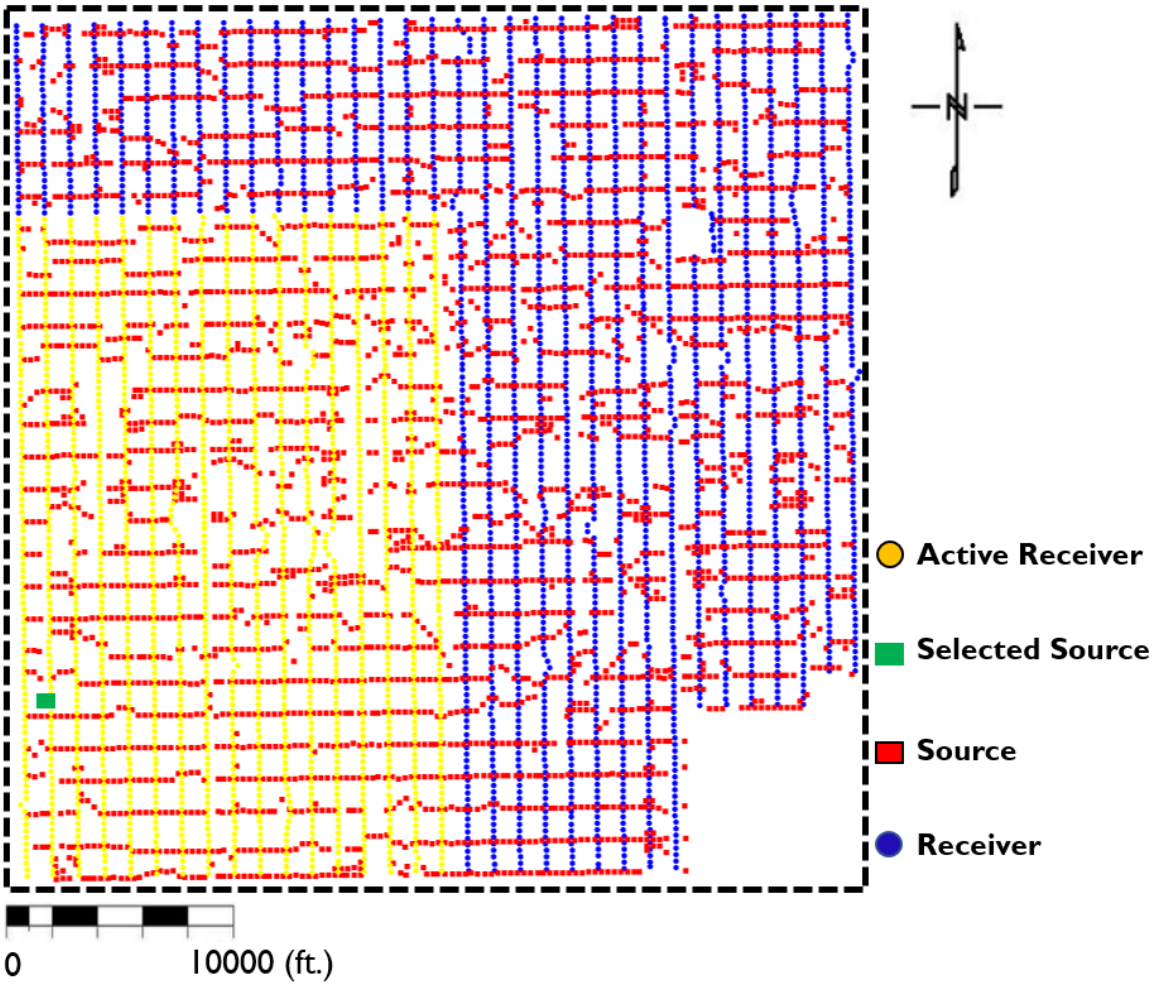

Figure 8: Common shot gather spatial geometry. A shot gather represents a set of seismic traces that correspond to a complete source (vibroseis) sweep. The active receivers corresponding to the shot are represented as yellow circles.

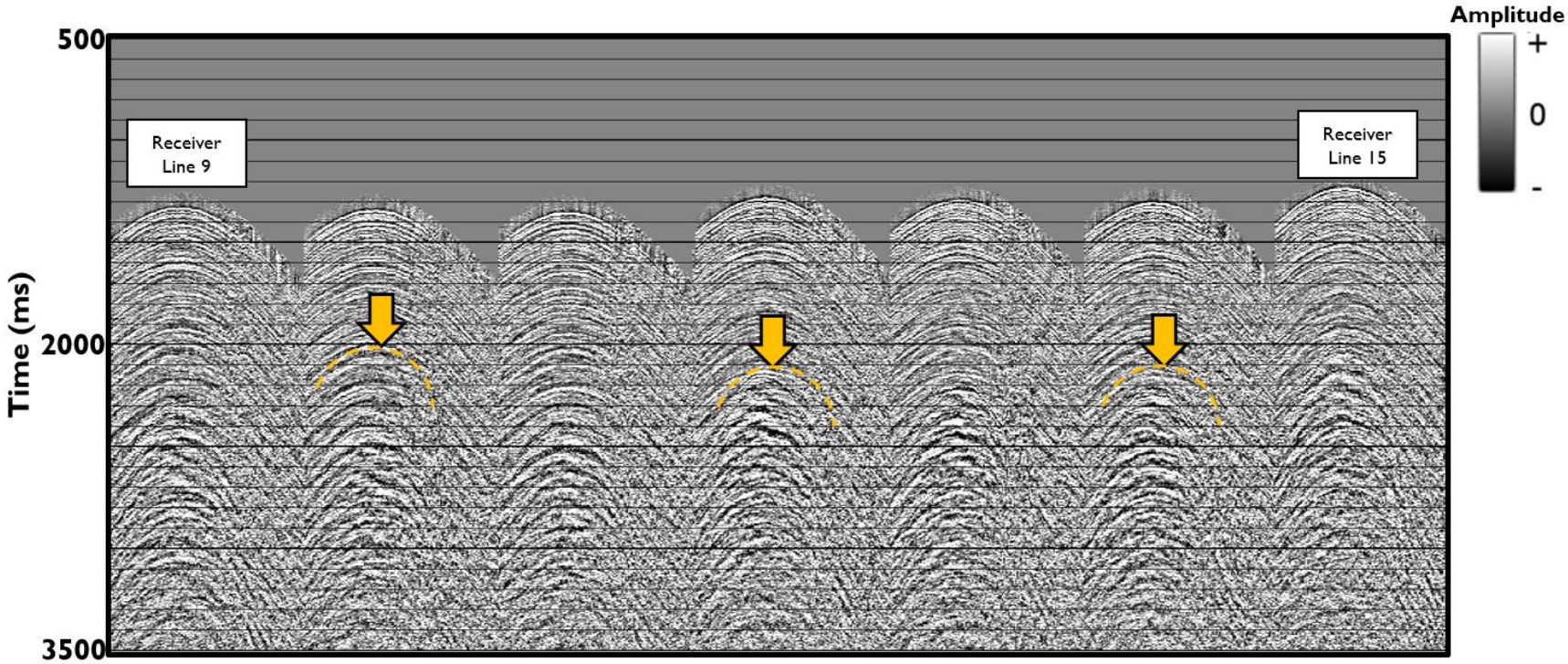

Figure 9: The common shot gather corresponding to the green source shown in Figure 8. The active receivers fall along 17 receiver lines, defining a "patch'. Several of these receiver lines forming the patch are displayed in Figure 9 where the ground roll travelling ''broadside'' to a receiver line exhibits hyperbolic moveout (in orange). This hyperbolic moveout is similar to that of reflection events of interest.

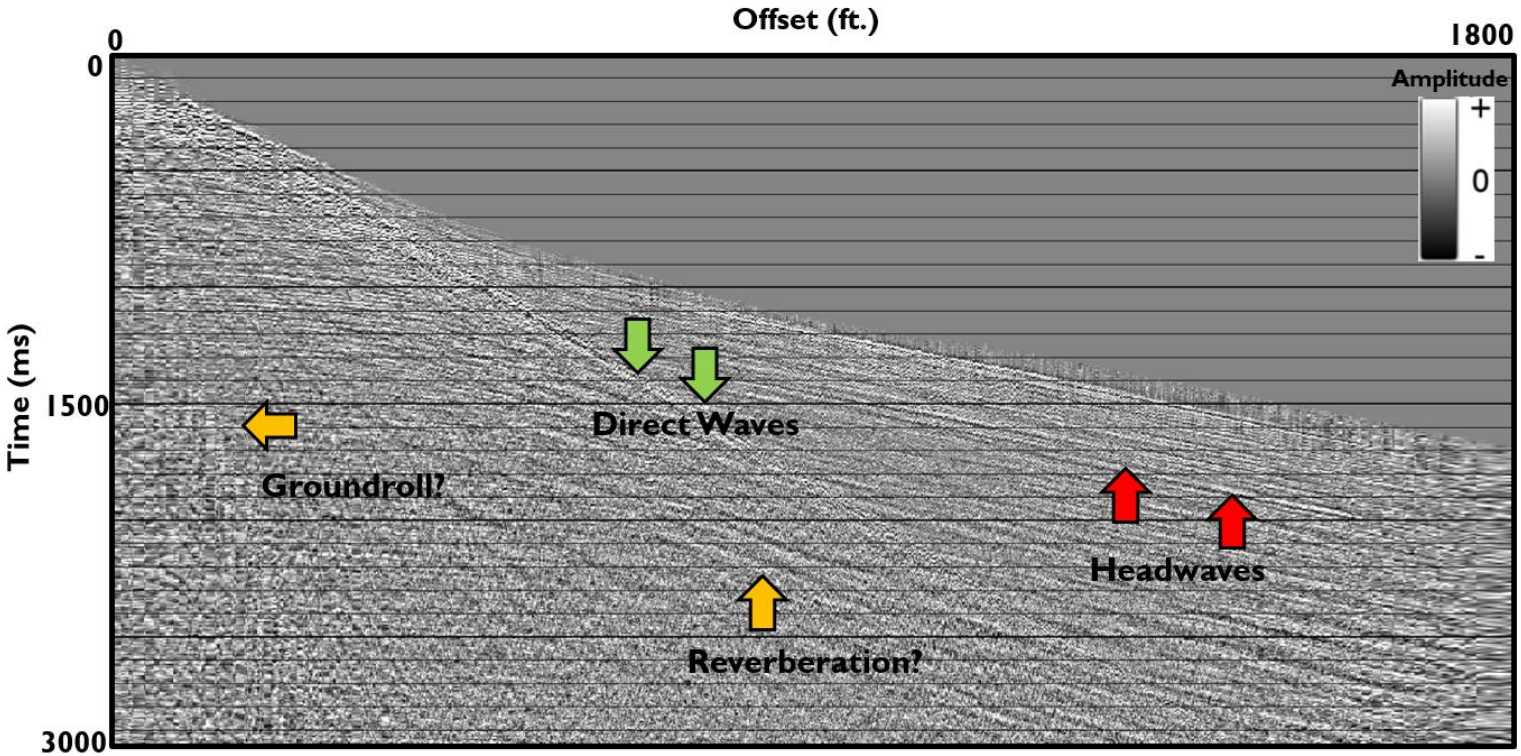

Figure 10: Image shows the entire shot gather sorted by source-receiver offset where the trace-to-trace separation is now irregular. Note the near linear moveout of ground roll and reverberations when the gather is deployed in this manner. However, adjacent traces in this sorted gather are not necessarily adjacent in (x, y) space making filtering difficult.

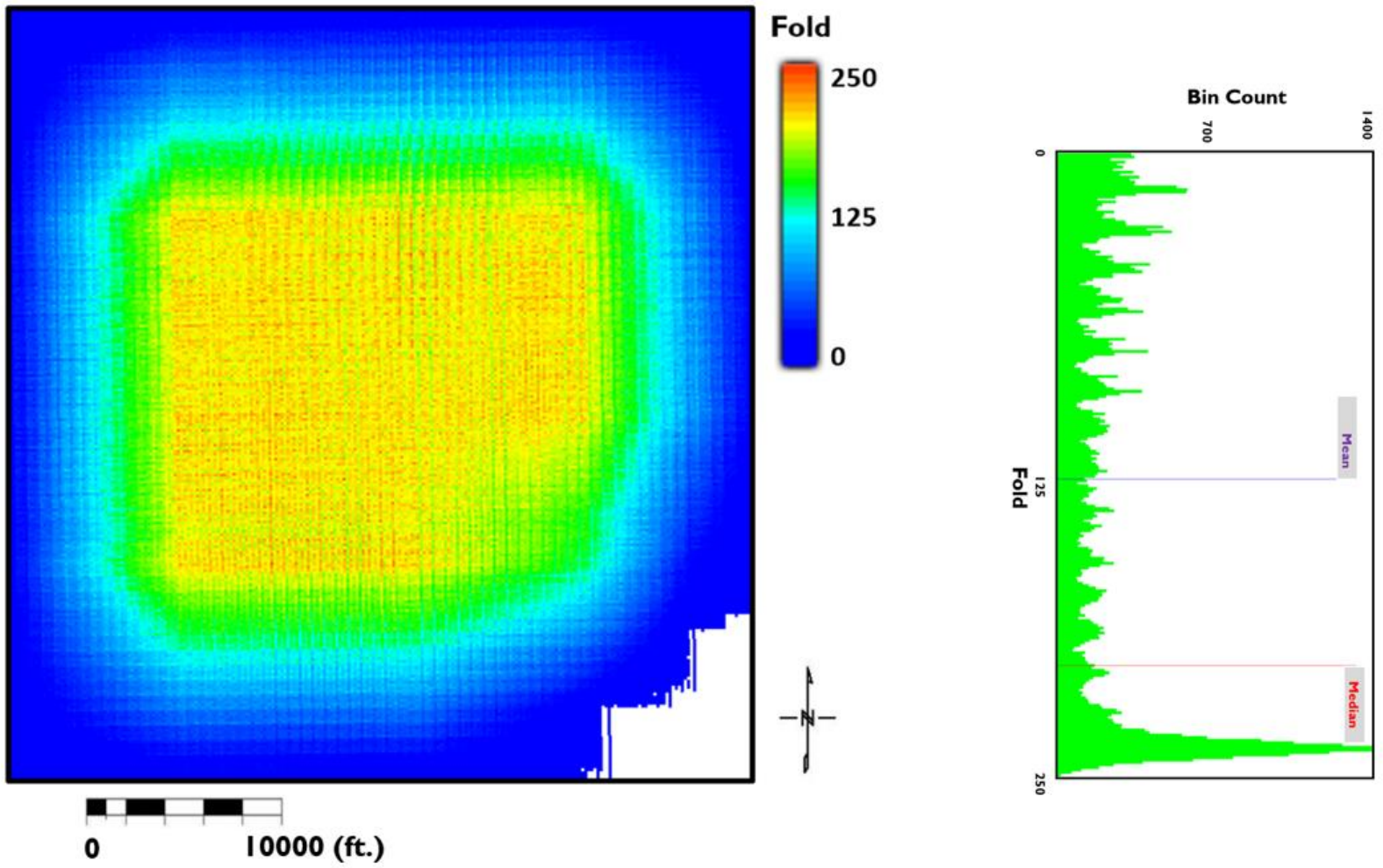

Figure 11: Fold map of the survey. The fold map represents the number of source-receiver midpoints in the CMP bins. The figure on the right shows the fold distribution of the survey. Maximum fold: 250. Average fold: 125

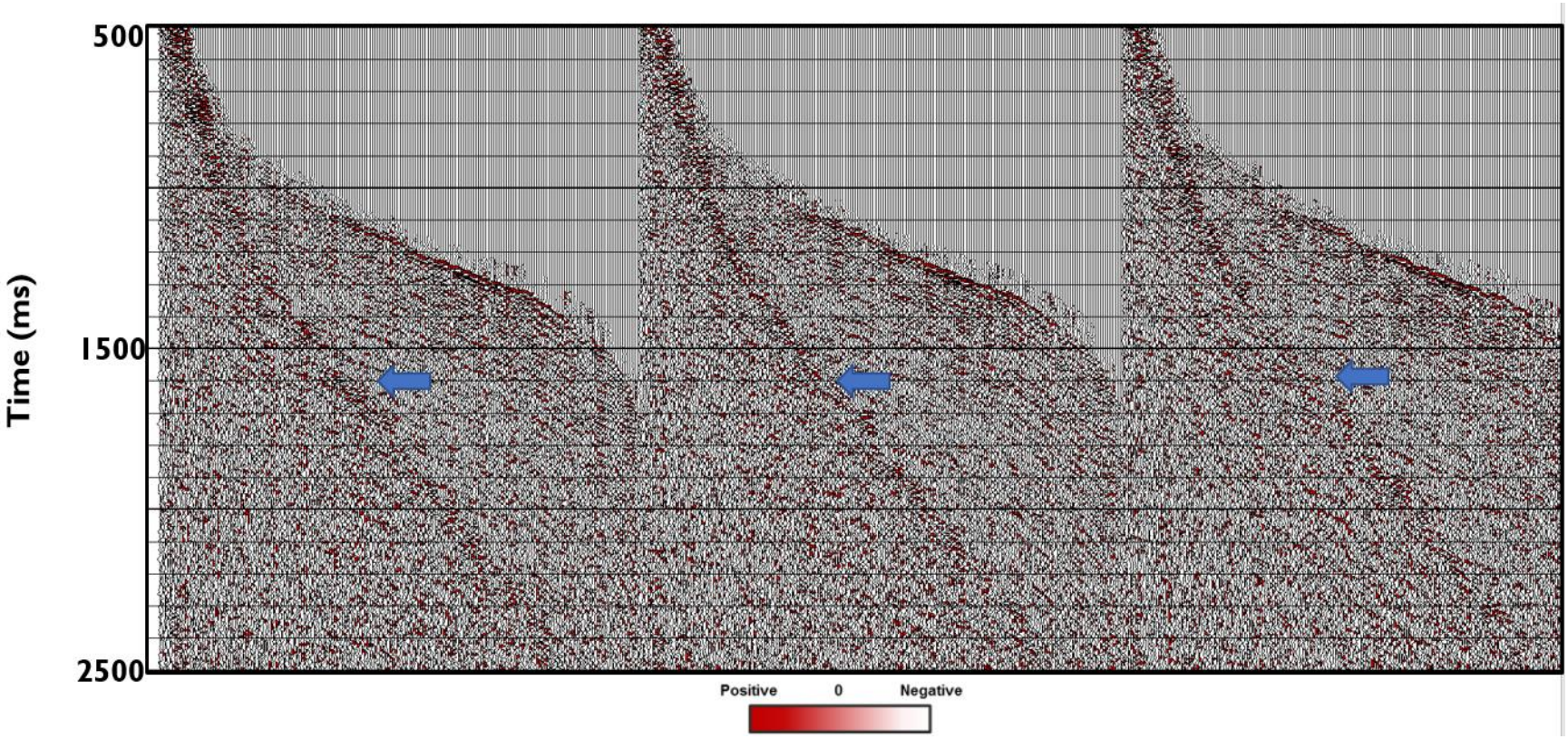

Figure 12: Three representative vendor processed common midpoint gather before the linear noise suppression with blue arrows indicating the area masked by the ground roll events

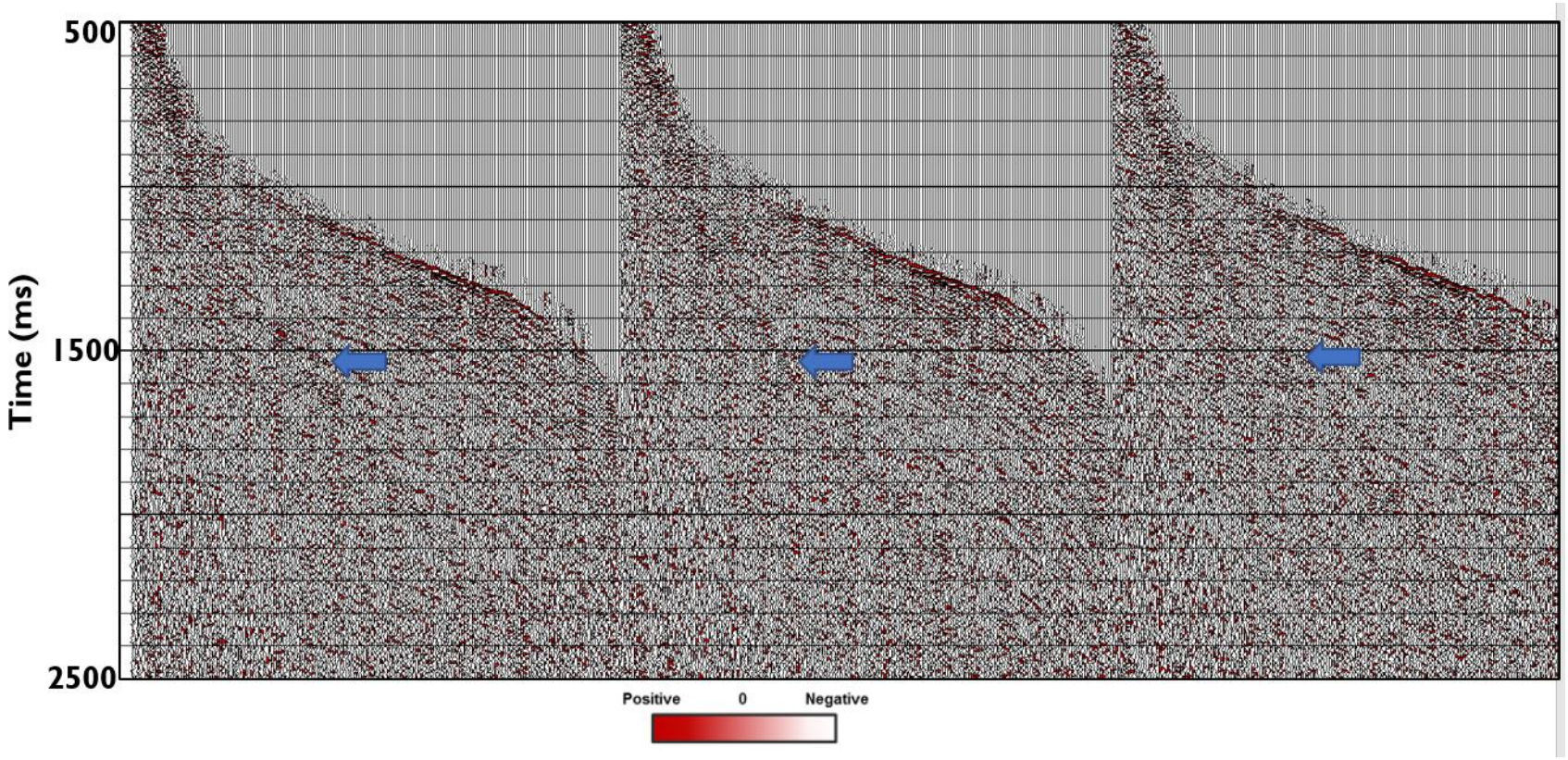

Figure 13: Common mid-point gather after the linear noise suppression workflow (LNR) was applied. The noise is attenuated compared to the original gather in Figure 12.

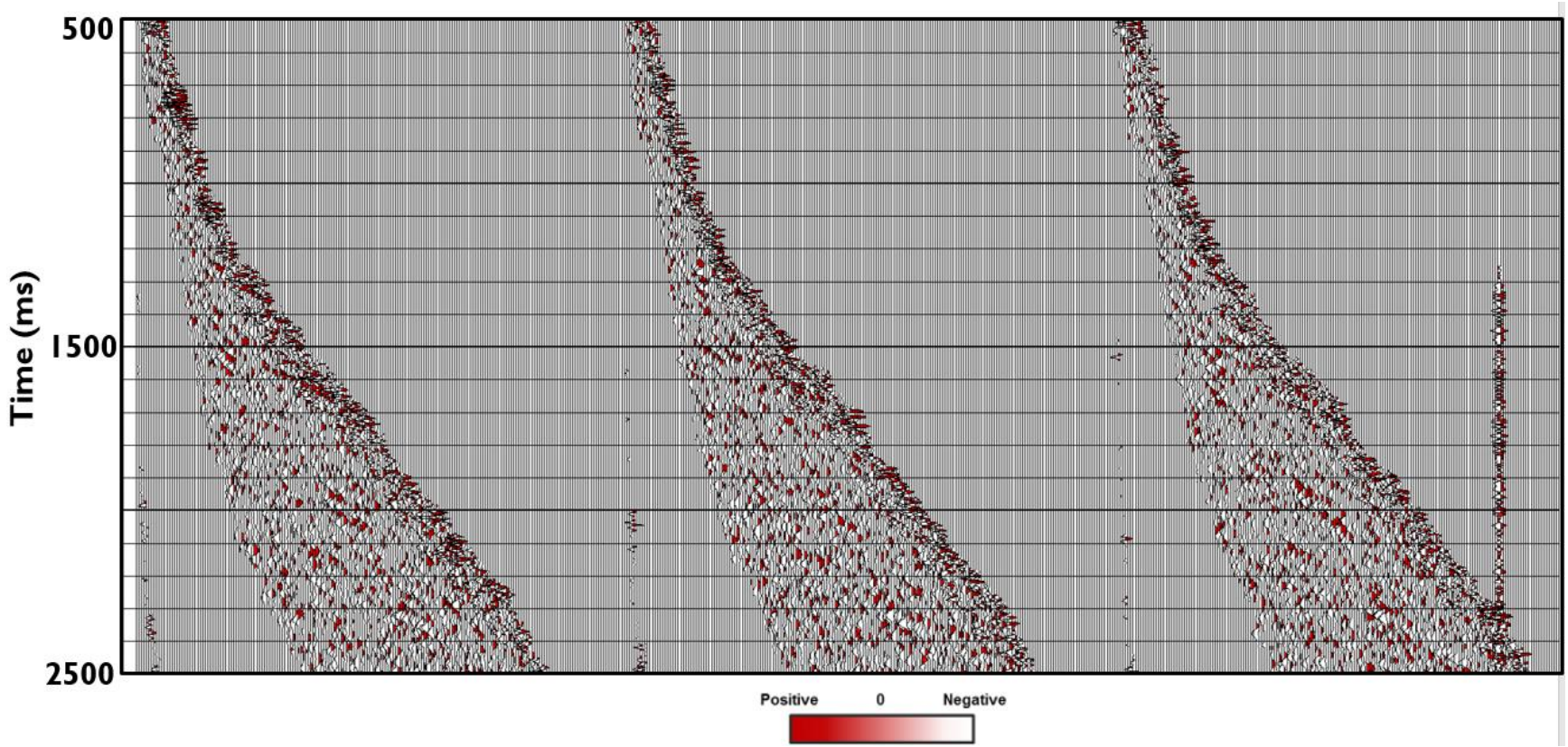

Figure 14: Common mid-point gather showing the difference between the gathers before and after the implementation of the linear noise suppression workflow. This difference also represents the isolated ground roll noise which is subsequently modeled and subtracted from the original data. The absence of hyperbolic reflections in these gathers serves as a quality control.

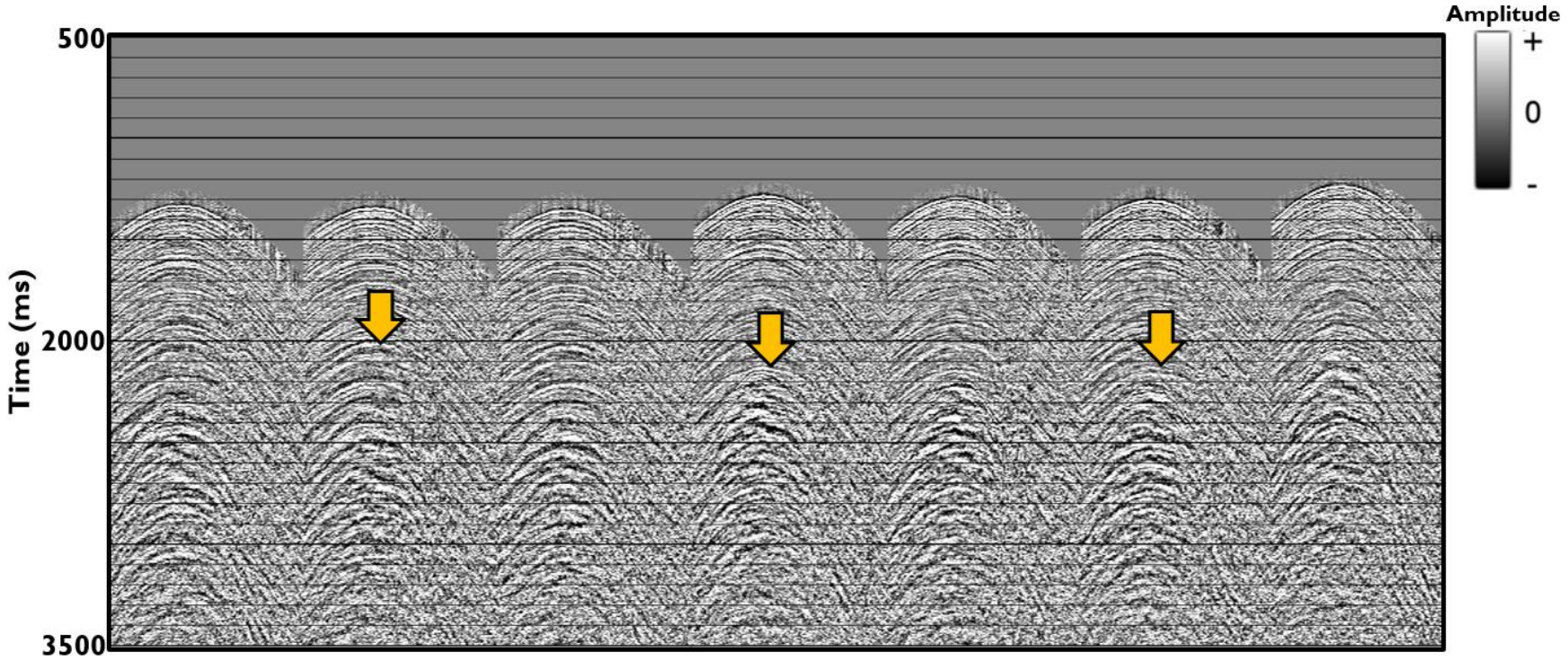

Figure 15: Seven of 16 receiver lines corresponding to a representative shot gather. This is a typical shot gather (shot vs. channel number) of the vendor-processed seismic data. Yellow arrows highlight the noise (ground roll) contaminated zone.

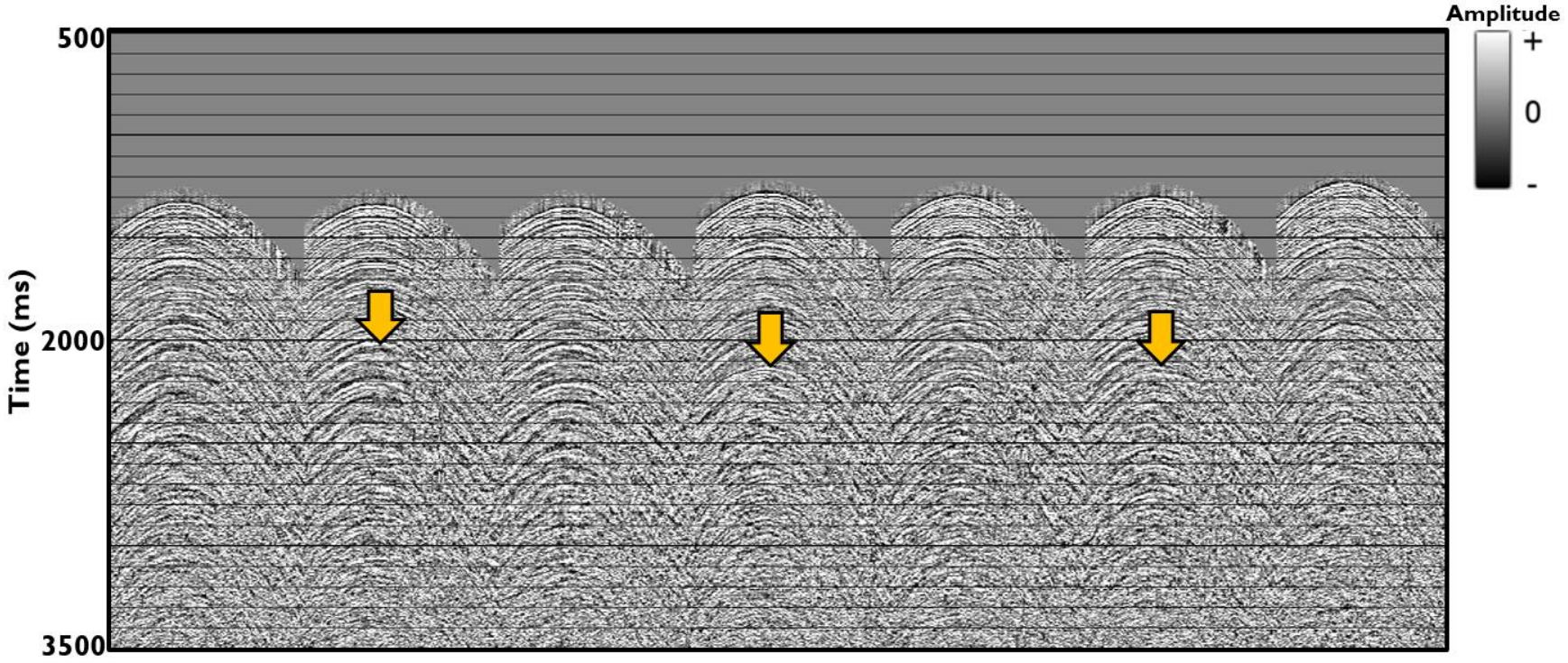

Figure 16: The same traces shown in the previous figure after the ground roll has been suppressed. Note that low frequency ground roll seem has now been thoroughly suppressed.

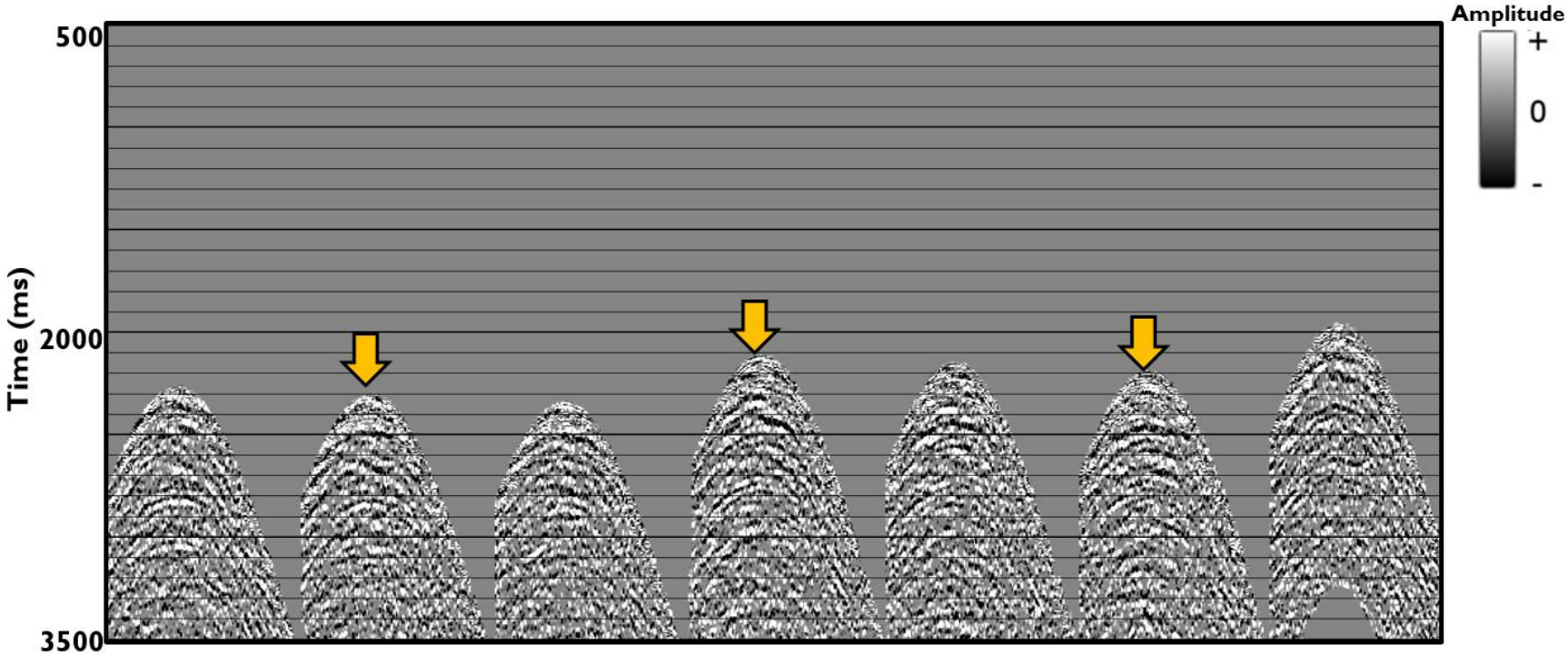

Figure 17: The same traces shown in the previous two figures showing the rejected ground roll.

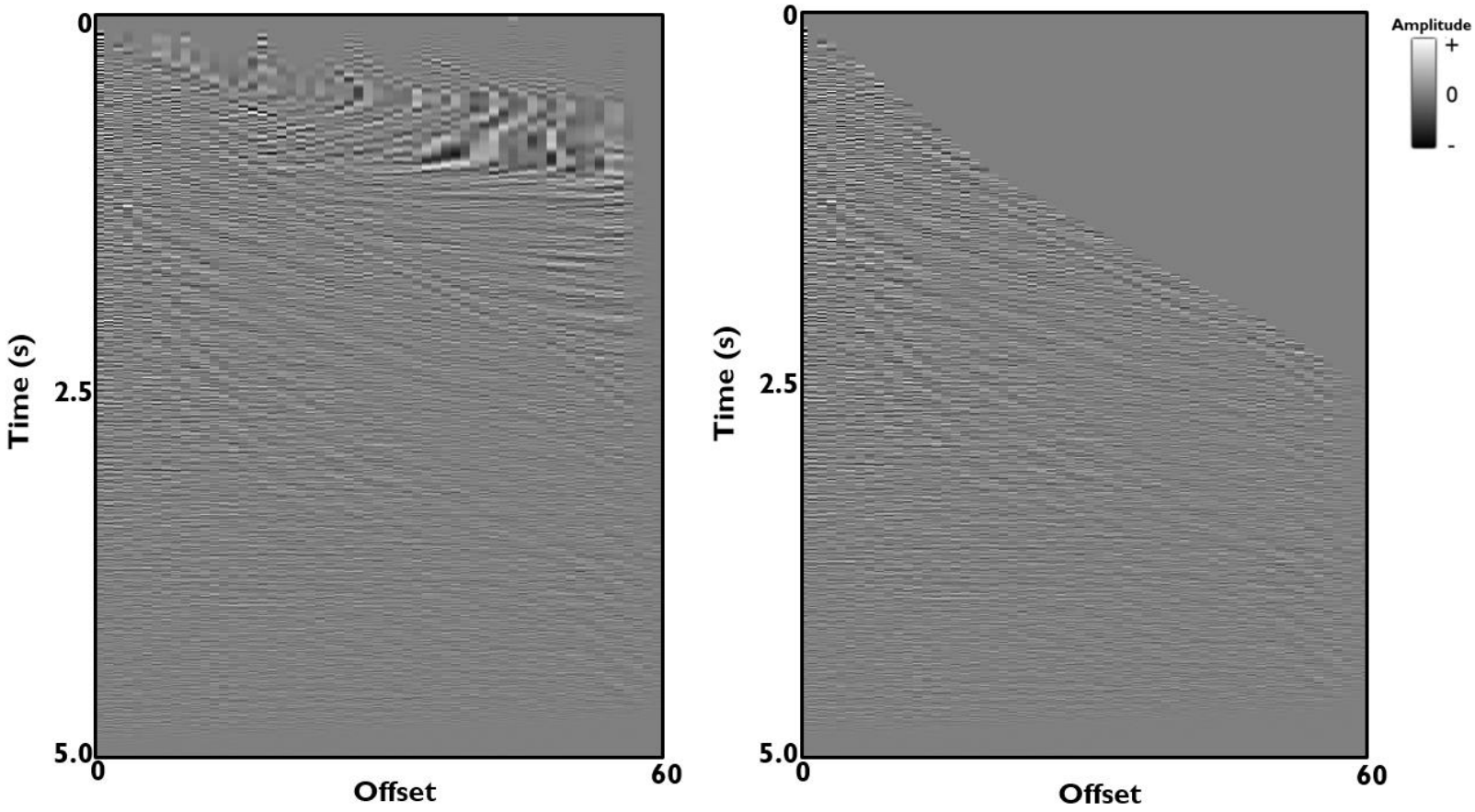

Figure 18: Prestack time migration result after the linear noise suppression without mute (left) and with mute (right) applied to remove stretched reflectors at far offsets.

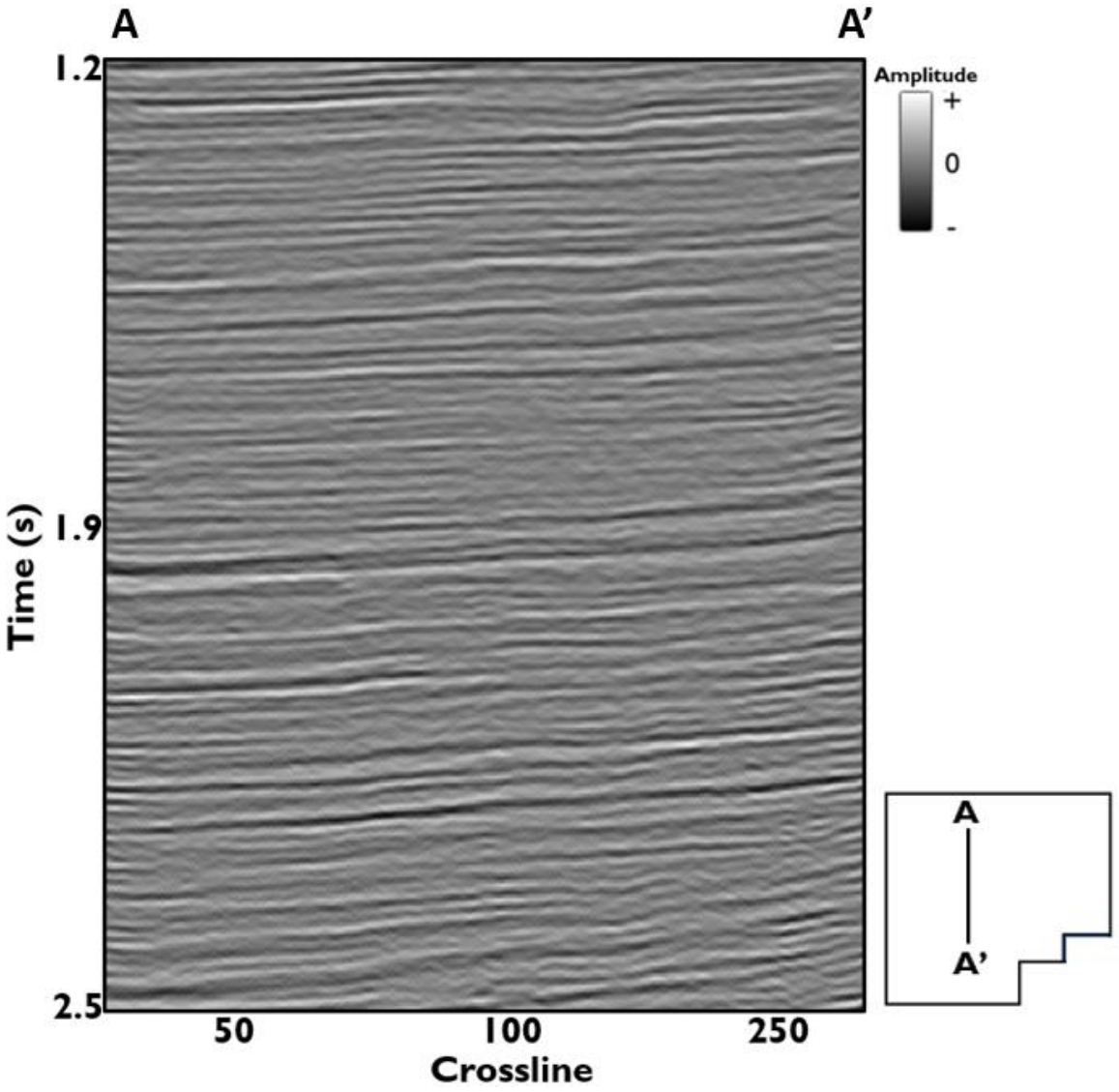

Figure 19: Line AA' through the stacked seismic volume. Notice appearance of some steeply dipping cross-cutting noise on the data suspected to have been introduced by migration process.

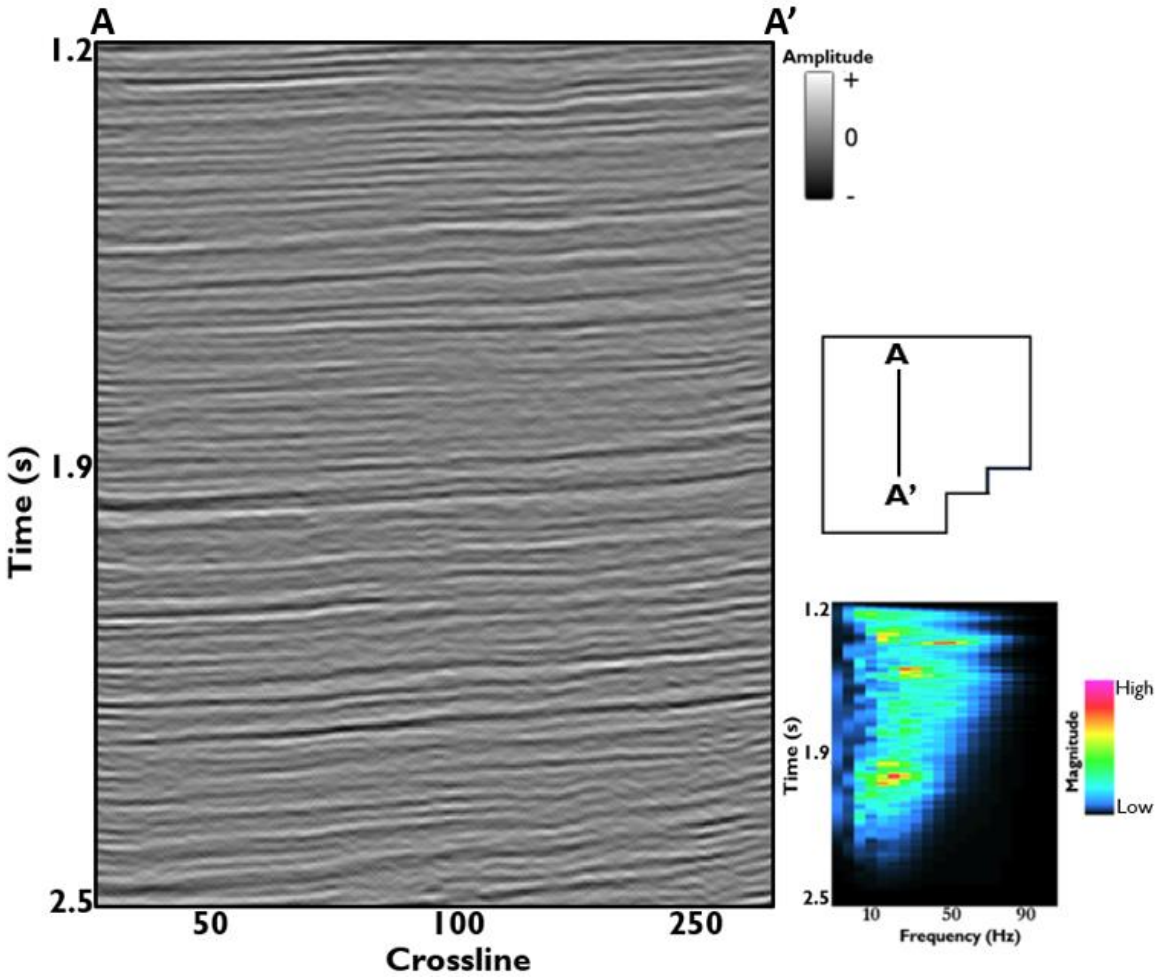

Figure 20: Line AA' through the unbalanced stacked seismic volume. Notice appearance of some steeply dipping cross-cutting noise on the data as well as the time variant frequency distribution on the right.

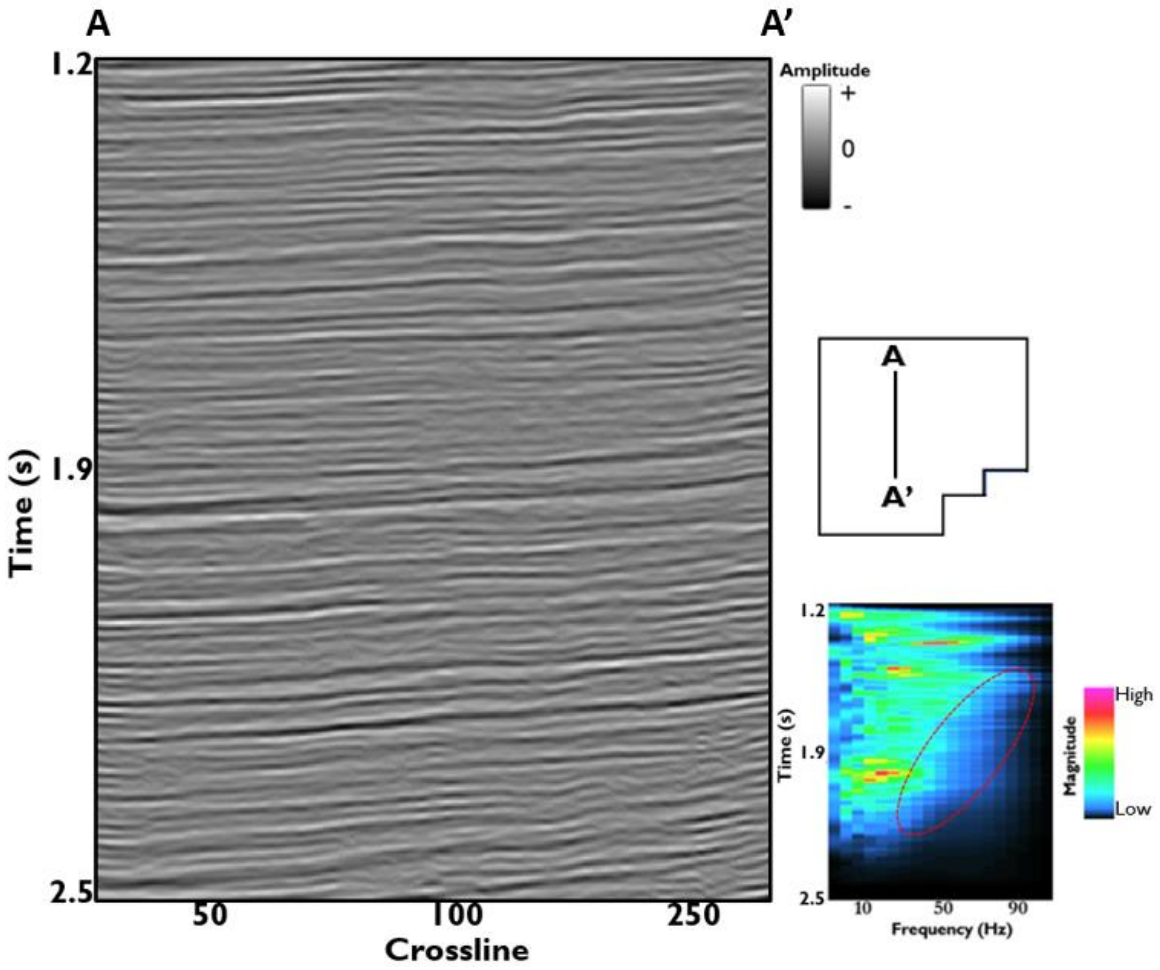

Figure 21: Spectrally balanced seismic volume with cross-cutting low frequency noise suppressed. The frequency spectrum of the data after spectrally-balanced data now shows higher frequency magnitudes when compared to the frequency content of the original unbalanced input data.

.

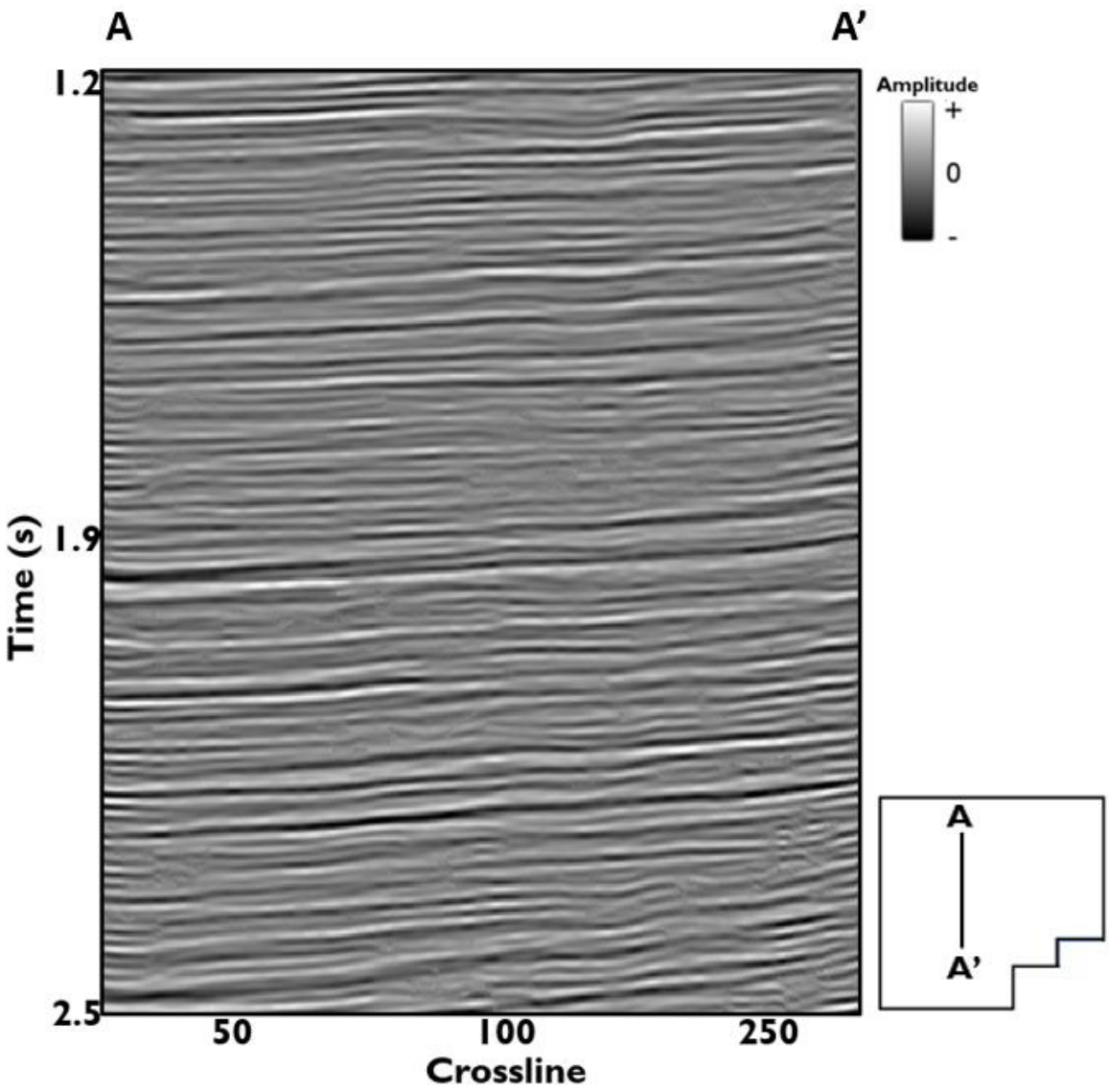

Figure 22: Final stacked migrated image after three iterations of structured oriented filtering. Notice the reflectors are now more continuous with most of the cross-cutting noise appearing in Figure 19 now mostly suppressed.

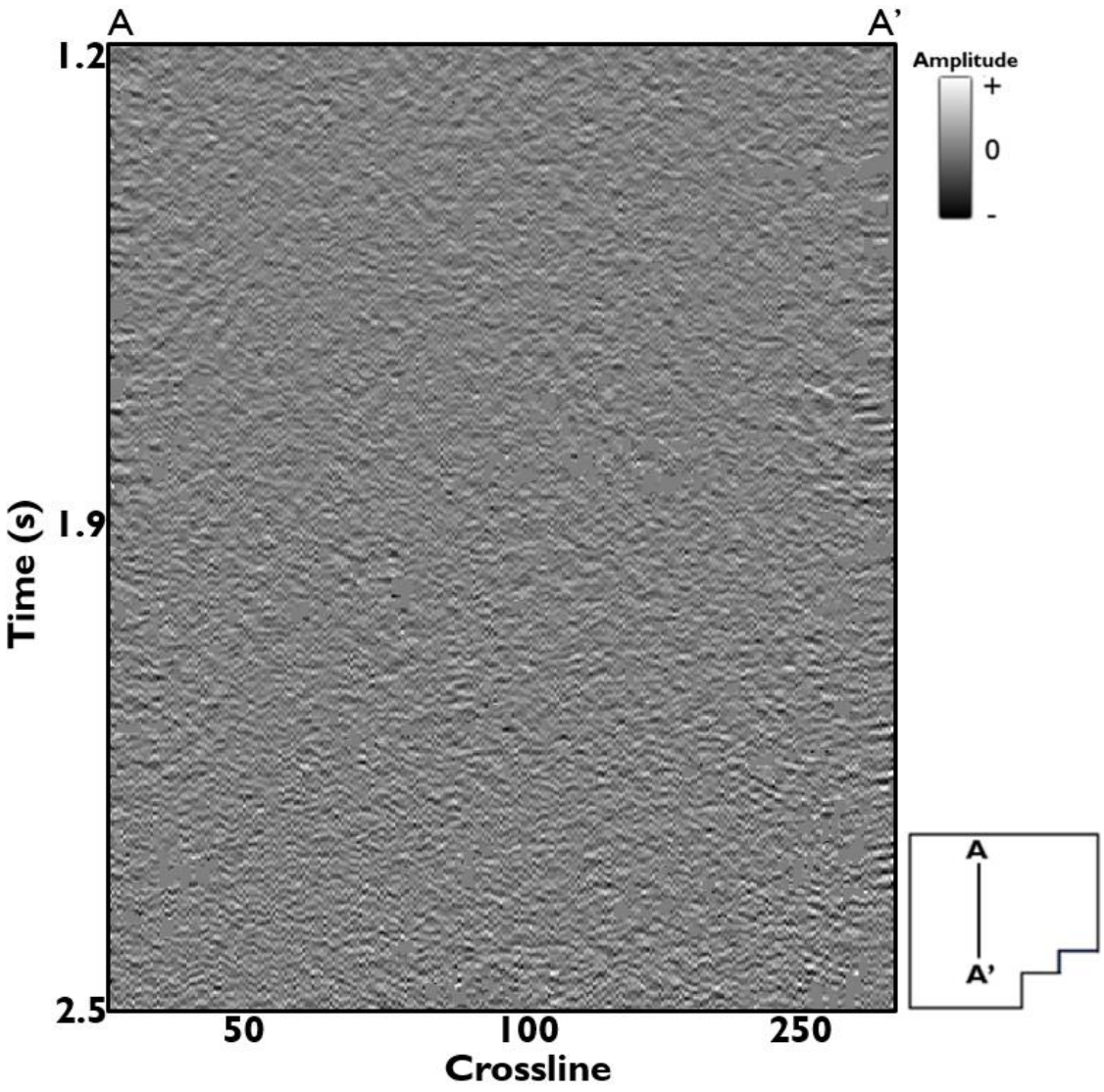

Figure 23: Vertical section showing the difference (rejected noise) between Figure 20 and 21. Notice the appearance of the suppressed cross-cutting noise.

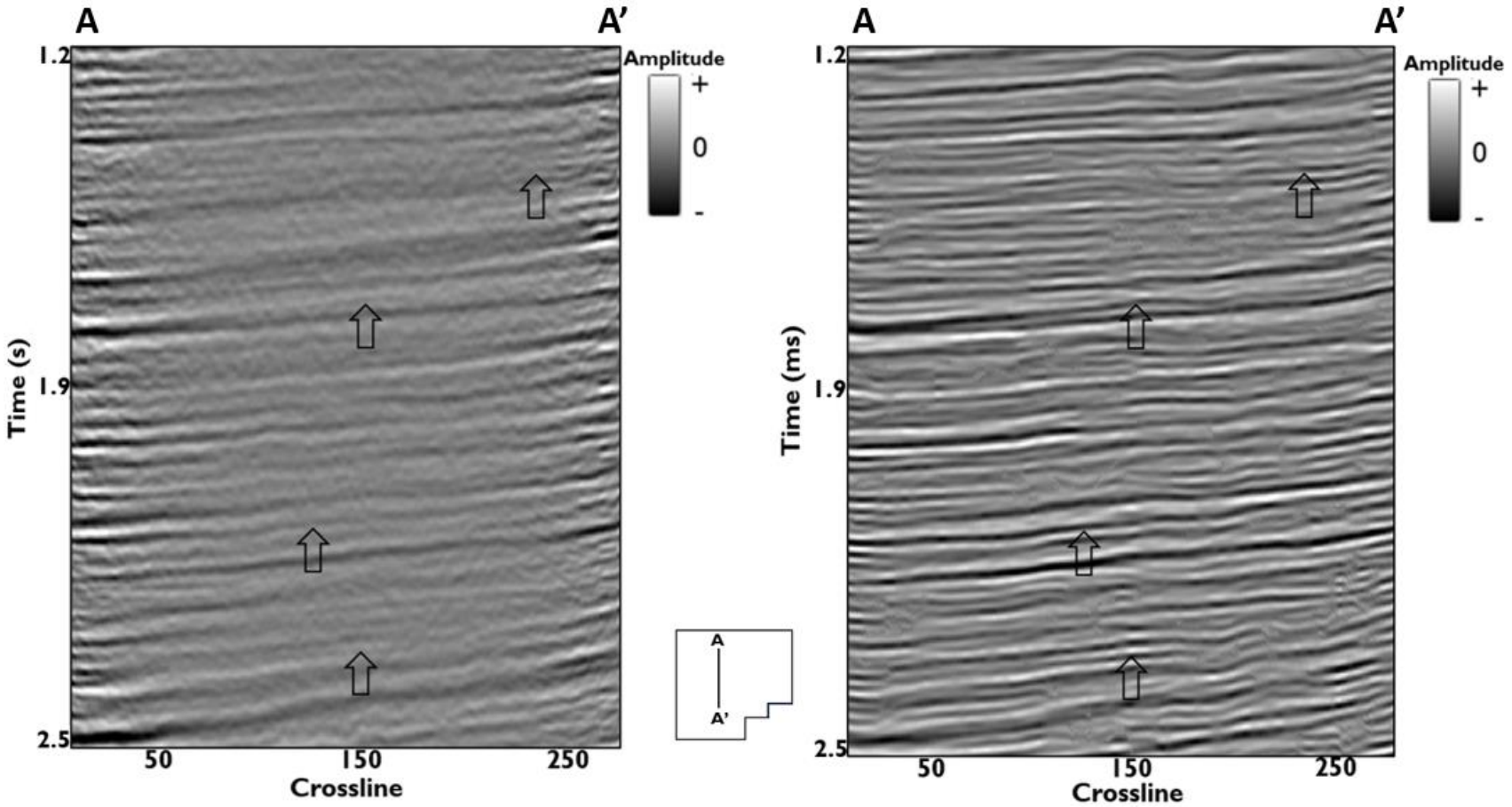

Figure 24: Line AA'through original (vendor) processed data (left) and the reprocessed final stacked volume. The reflectors on the reprocessed data are broadband and are more continuous. Arrows highlights major improvements on the data.

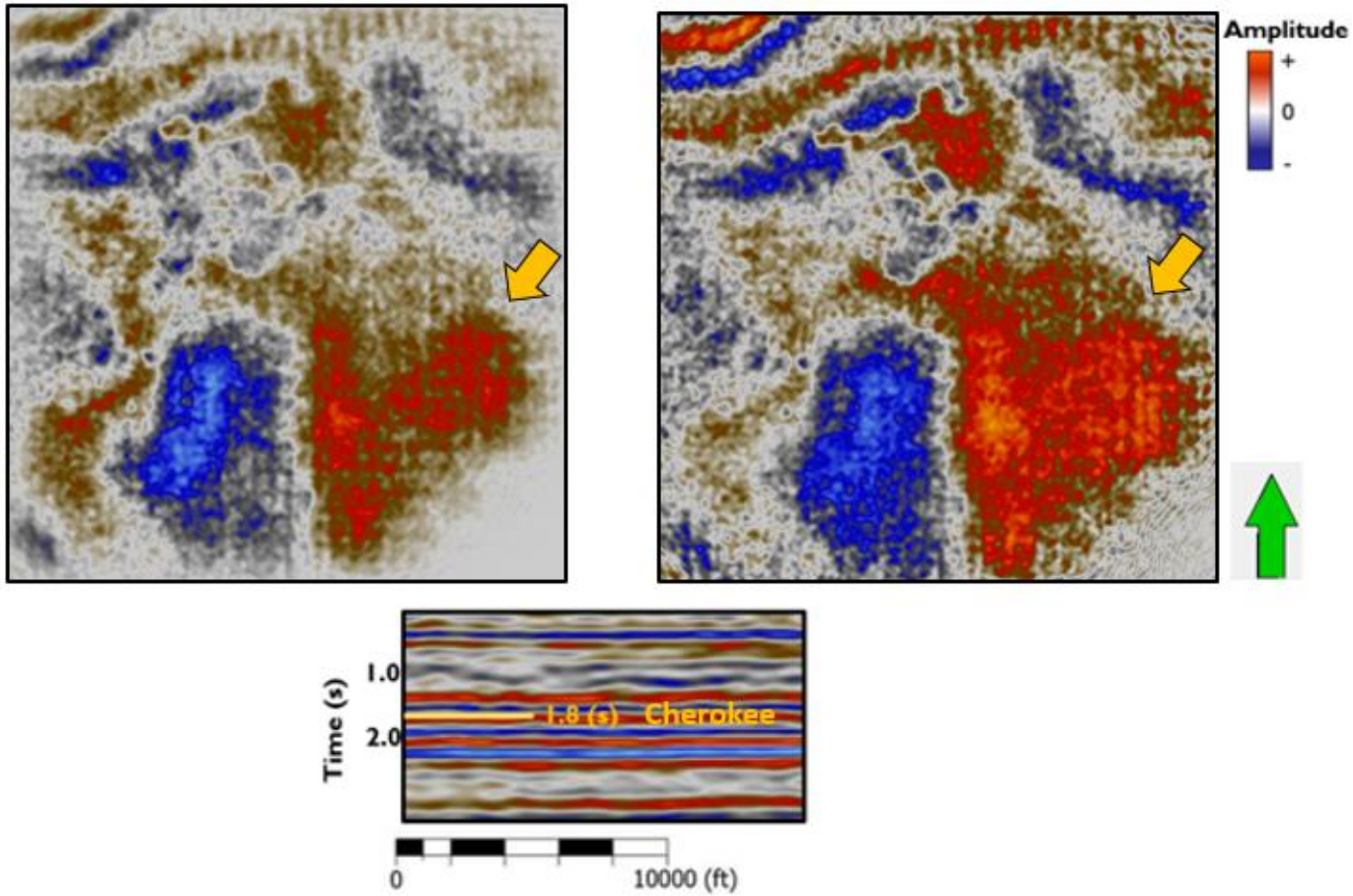

Figure 25: Time slice at 1.8 through the original (vendor) and reprocessed data at t = 1.8s (near the target formation). Here, the amplitudes are more continuous and foot print better suppressed.

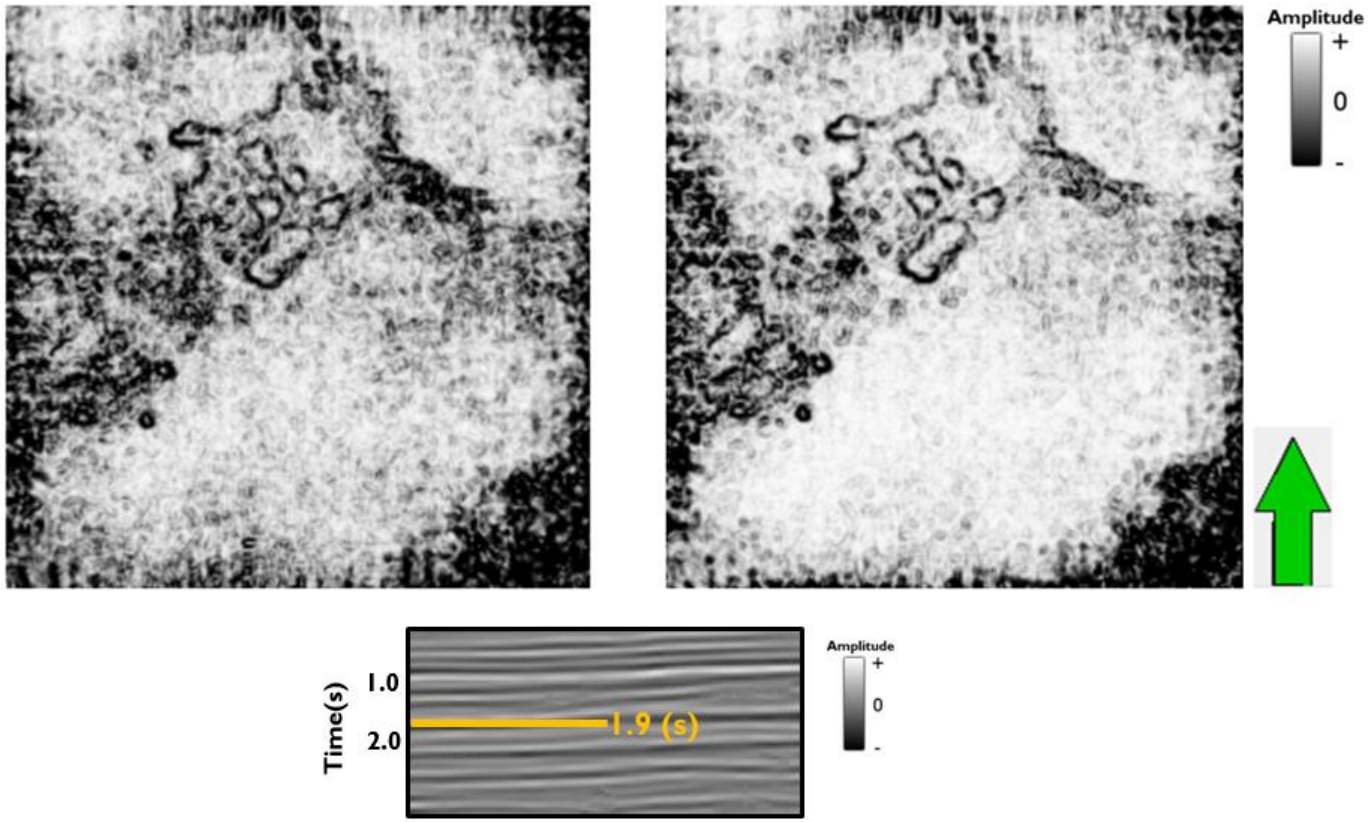

Figure 26: Coherence time slice through the original (vendor) and reprocessed data at t = 1.8s (near the target formation). Here, the amplitudes are more continuous and foot print better suppressed.

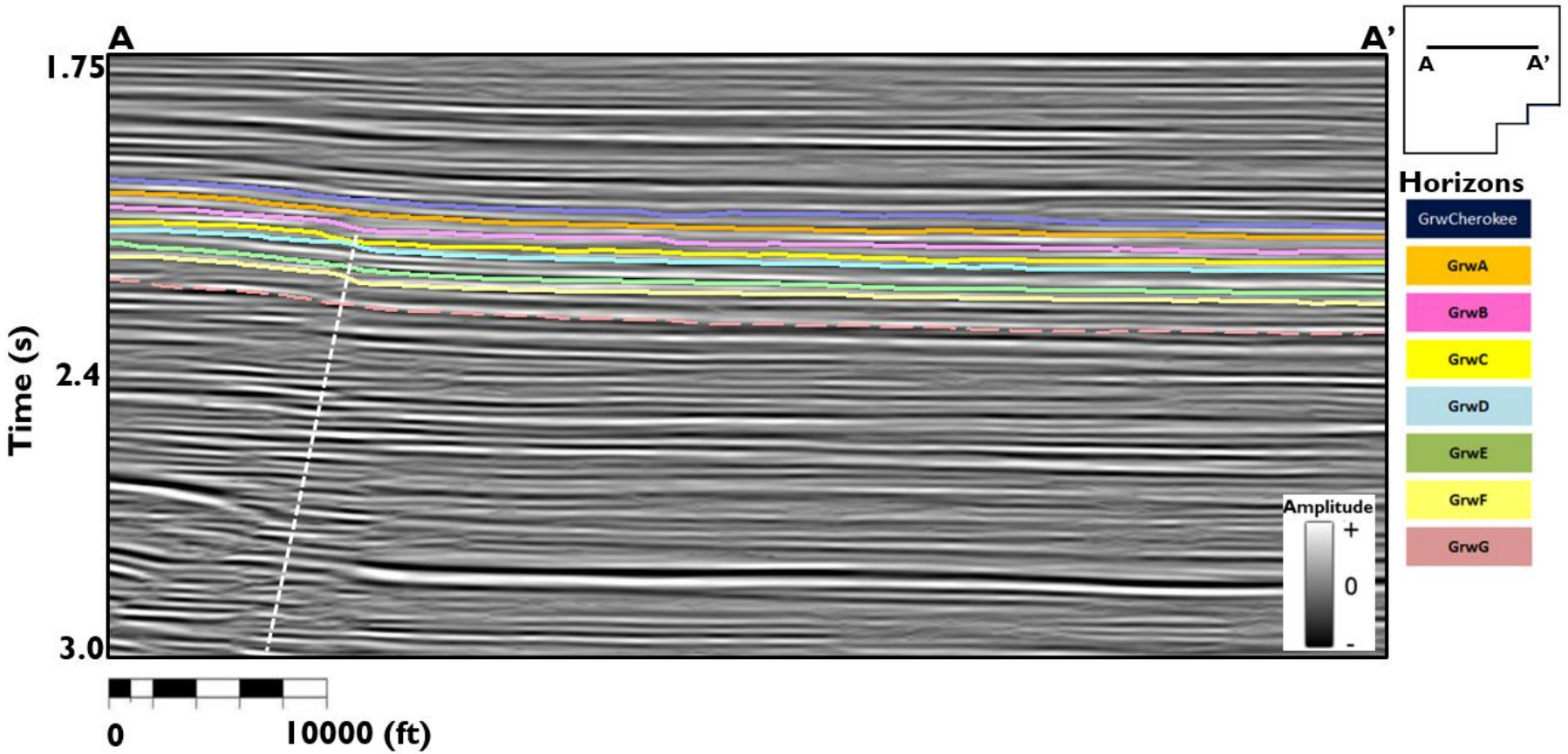

Figure 27: Vertical section from A-A' showing key Granite Wash horizons. The reflectors thinning towards the west indicates an evidence of syndepositional tectonics. The dashed line shows the major fault in the survey.

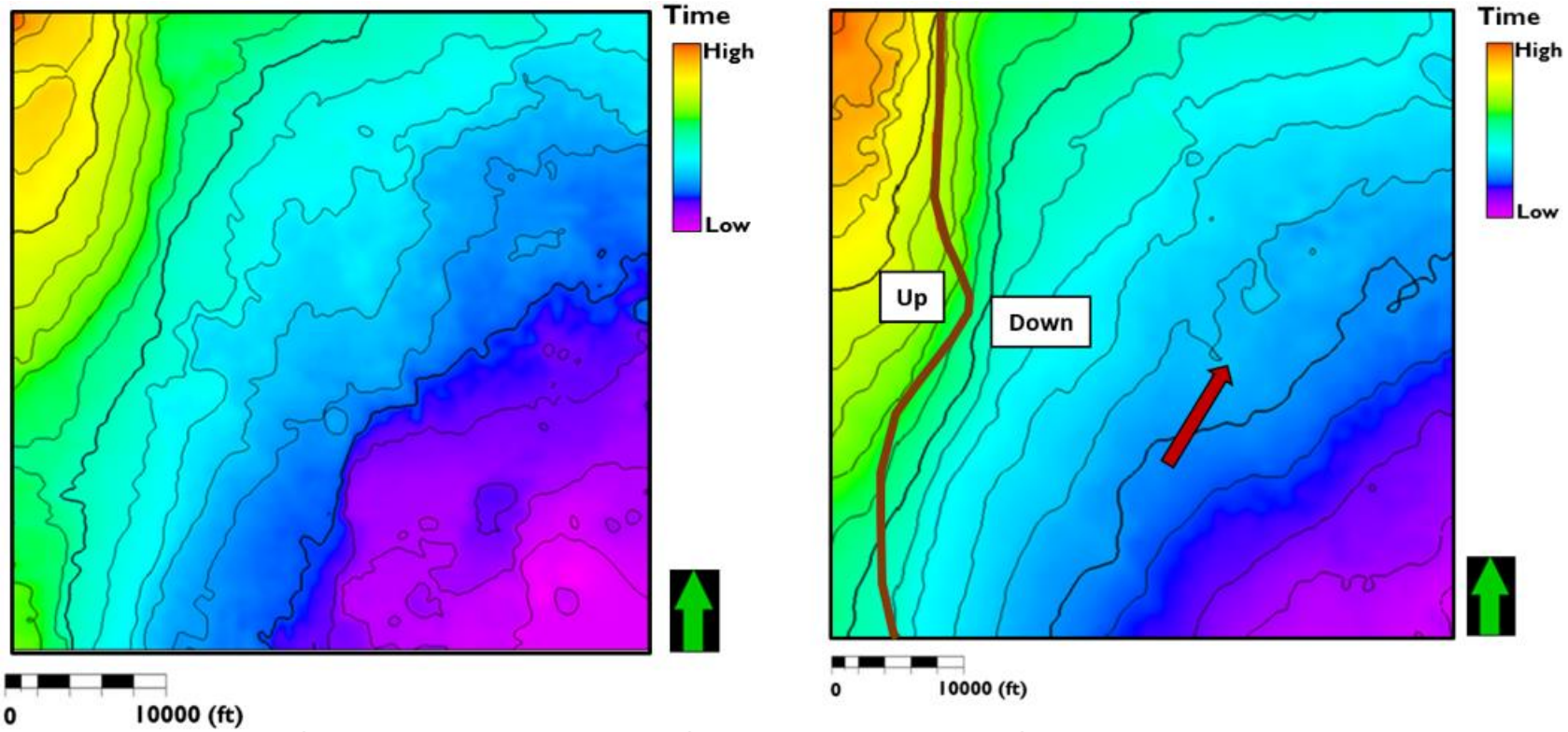

Figure 28: Time structure map of the Cherokee Granite Wash (left) and the Granite Wash-G formation (right). The red arrow indicates the paleo-direction of the sediments as they are being moved from SW to NW. The red line shows the major fault path within the survey.

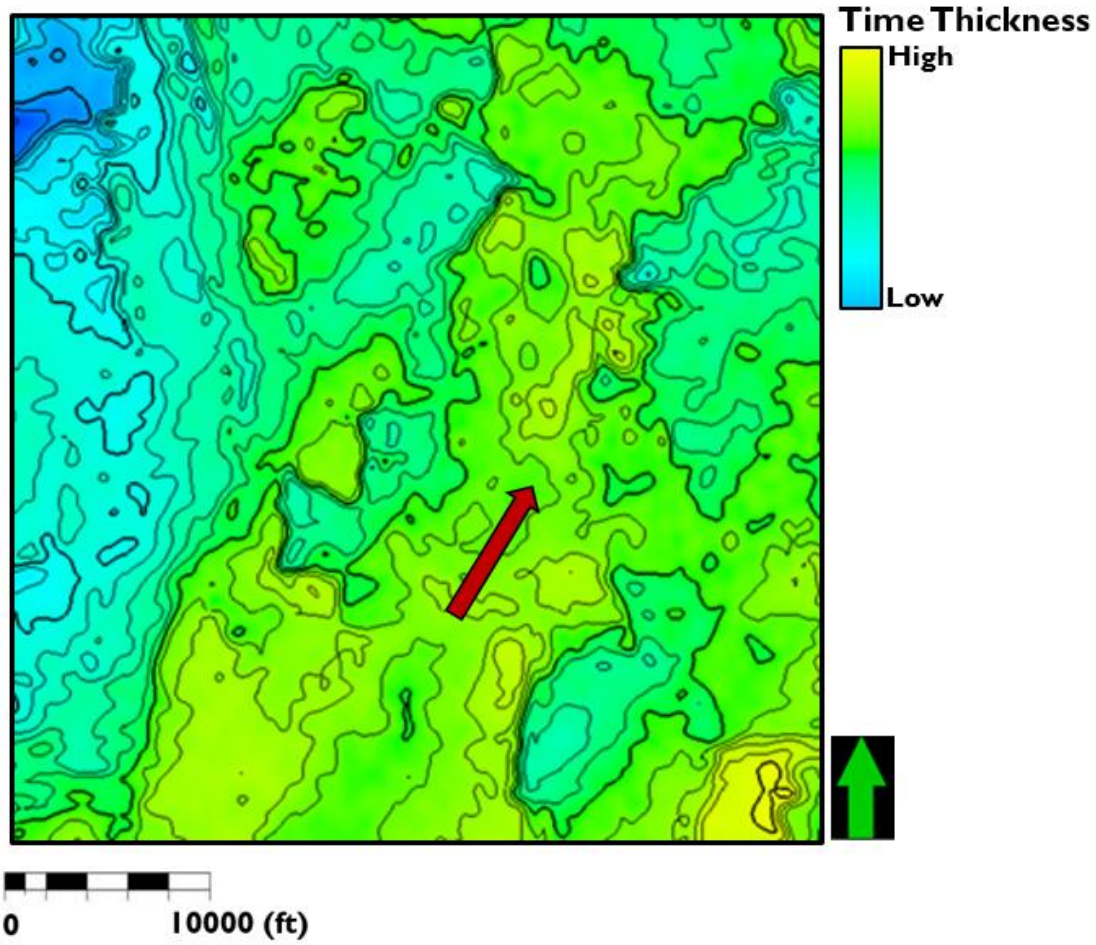

Figure 29: Isochron map of the Cherokee-GRWG interval. Sediments deposition to the south, where the sediments are thickest, could be associated with the accumulation of alluvial fans that thins as the fan progrades towards the deeper portion of the basin.

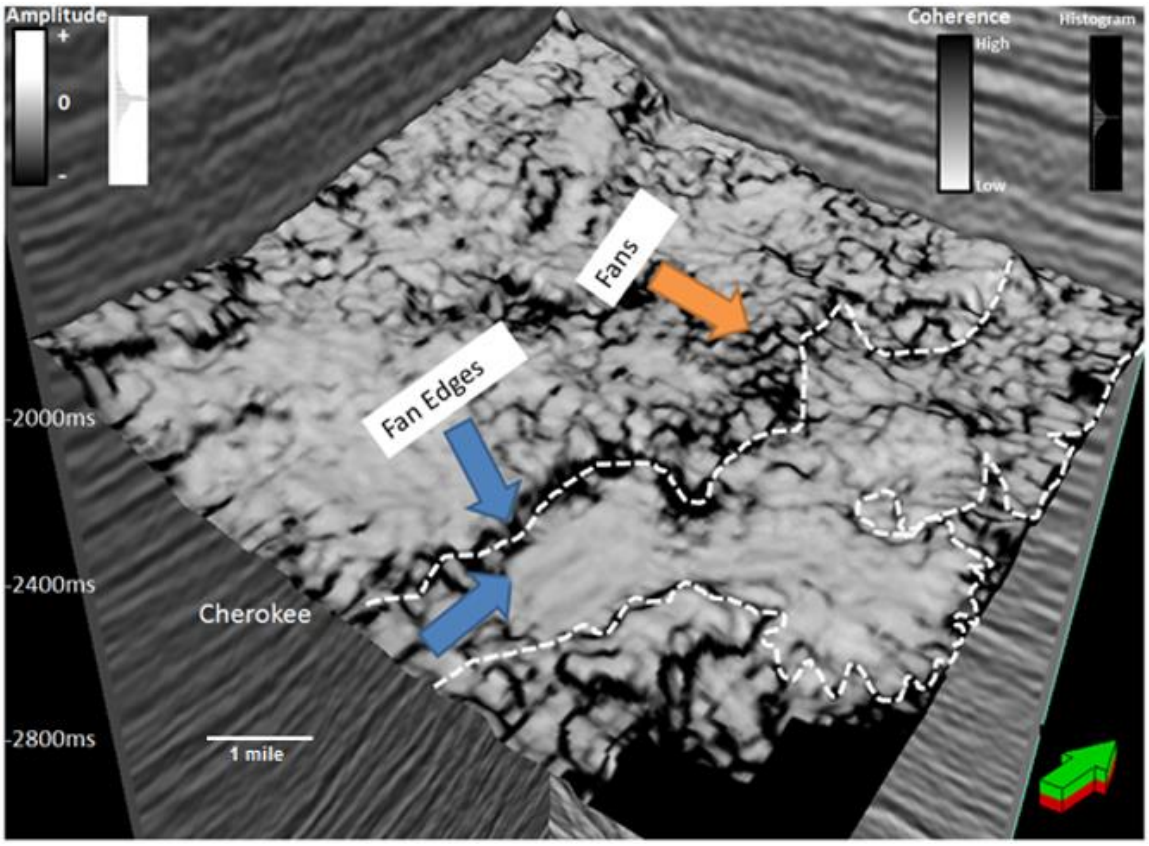

Figure 30: Coherence attribute extracted along the top of the Cherokee wash. Arrows indicate fan, faults and canyon edges. Abrupt changes in waveforms are generally indicative of faults as well as changes in depositional features.

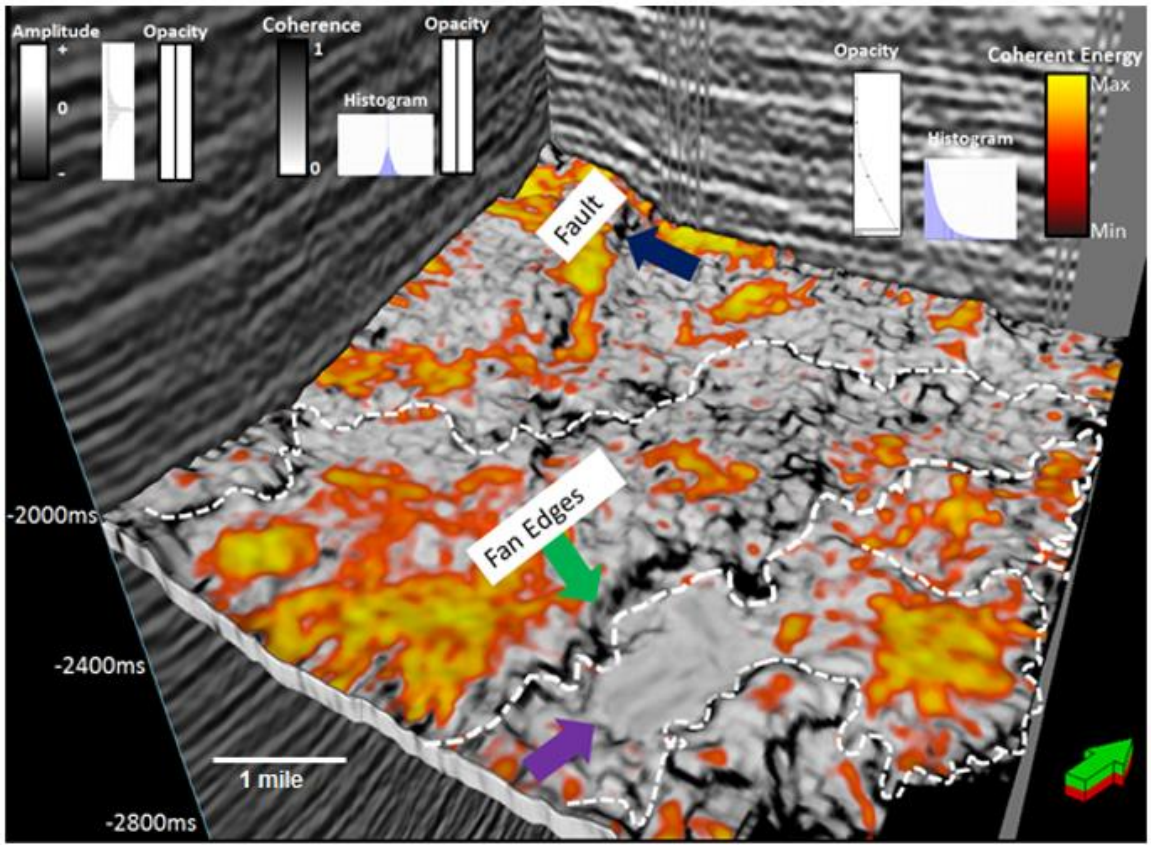

Figure 31: Co-rendered image of coherence attribute with the coherent energy. Note that high relief areas in the image have high coherent energy whereas fan/fault edges have low coherence energy.

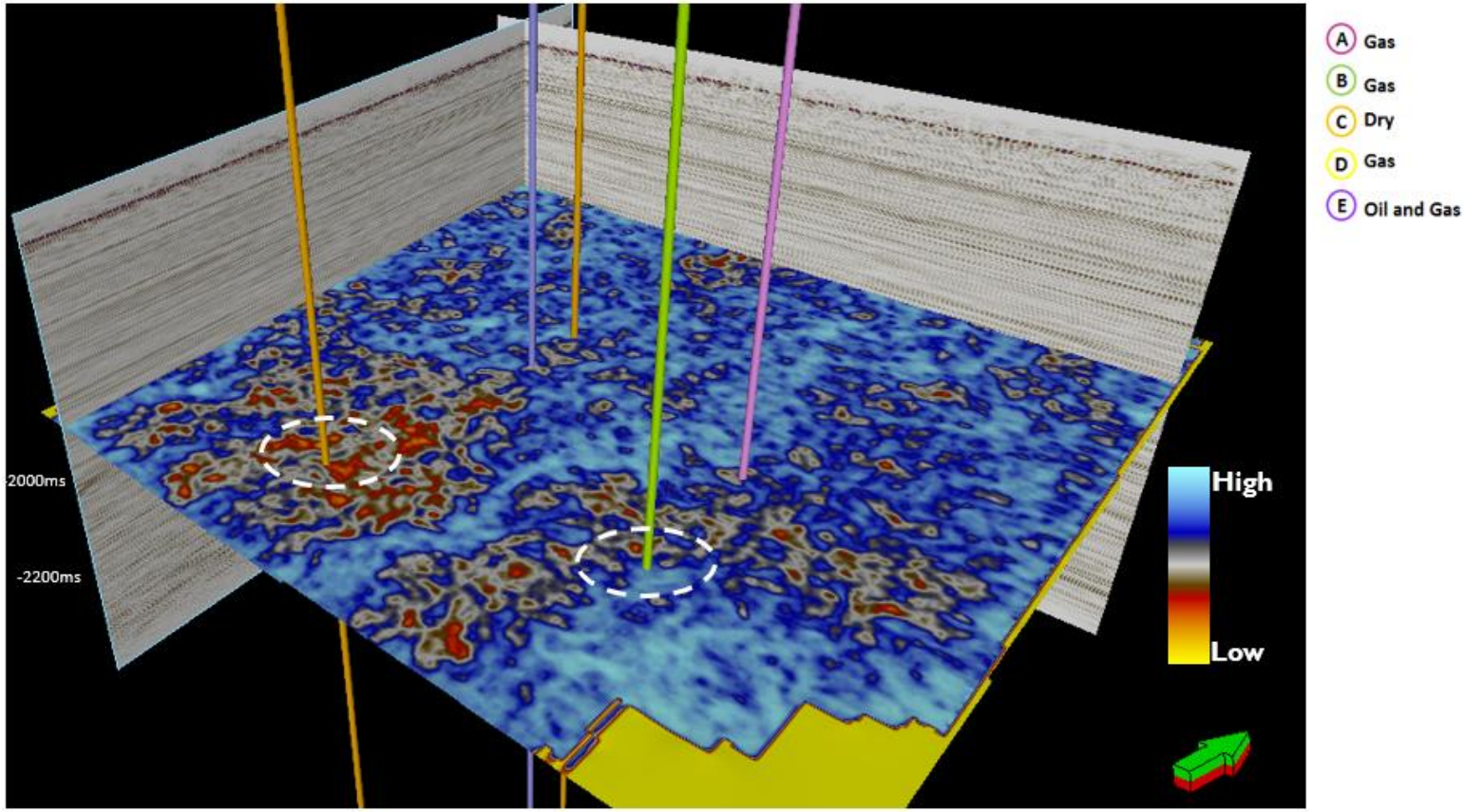

Figure 32: GLCM entropy attribute: Seismic texture attributes indicate areas that correlate to gas wells. Gas bearing zones indicate high energy, low entropy, and high homogeneity. Oil bearing areas show moderate energy and homogeneity and low entropy values.

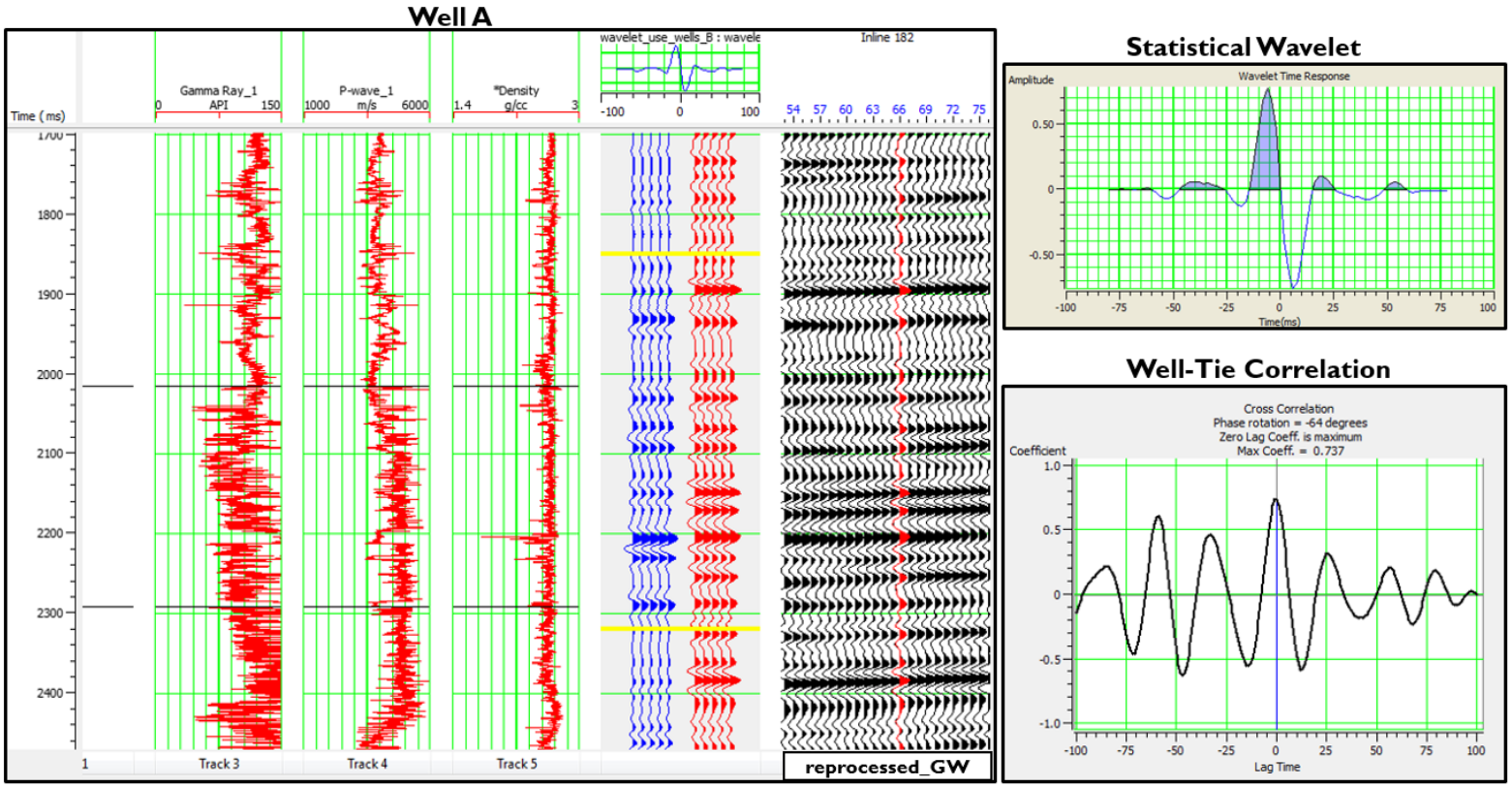

Figure 33: Density and P-wave logs, synthetic seismogram, and extracted seismic trace of the **reprocessed** data. There is a good correlation between the synthetic and extracted seismic traces (correlation = 0.737).

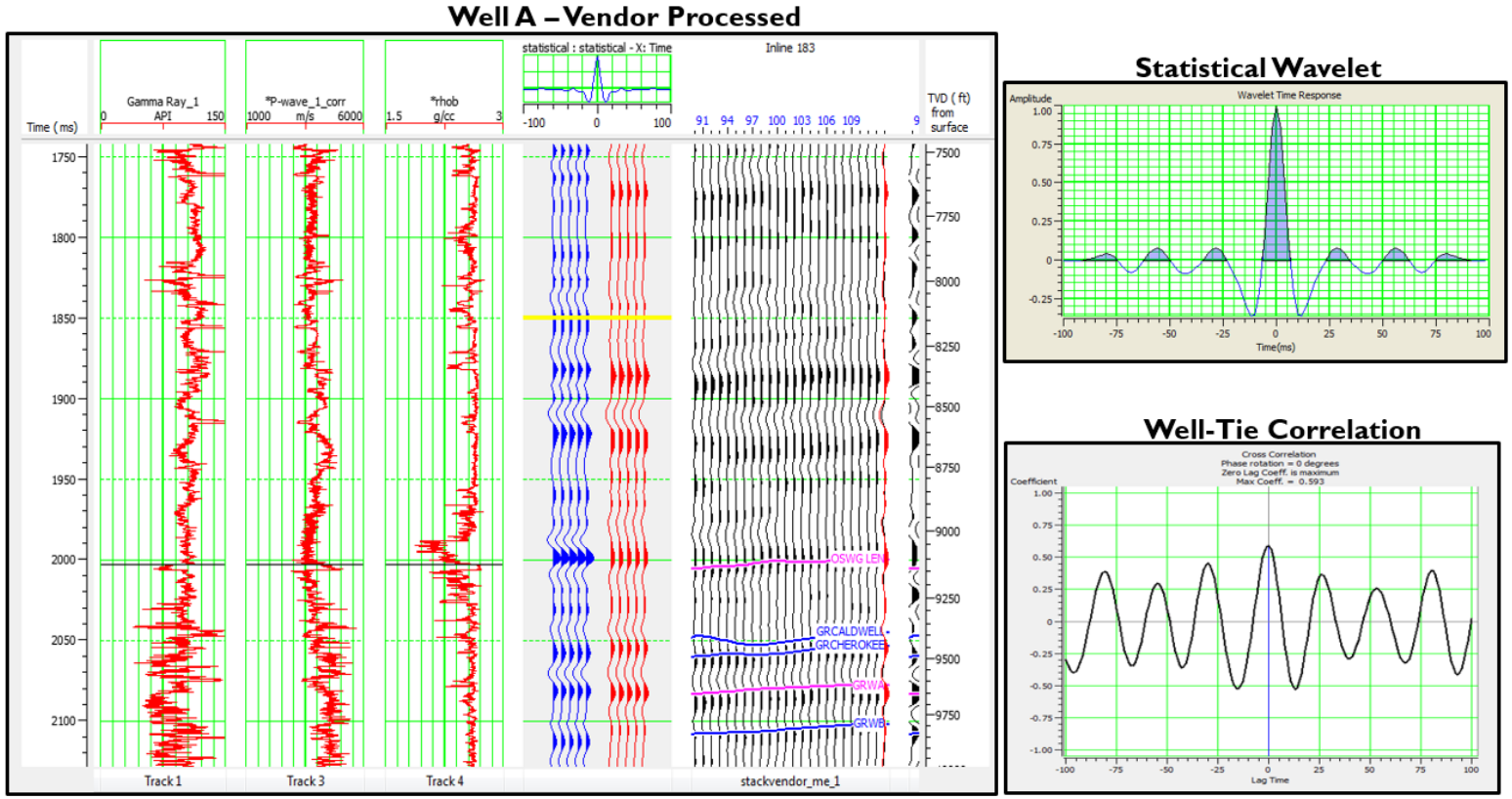

Figure 34: Density and P-wave logs, synthetic seismogram, and extracted seismic trace of the **vendor-processed** data. The correlation obtained is lower (0.593) compared to the value obtained (0.757) when the wells are tied to the reprocessed data.

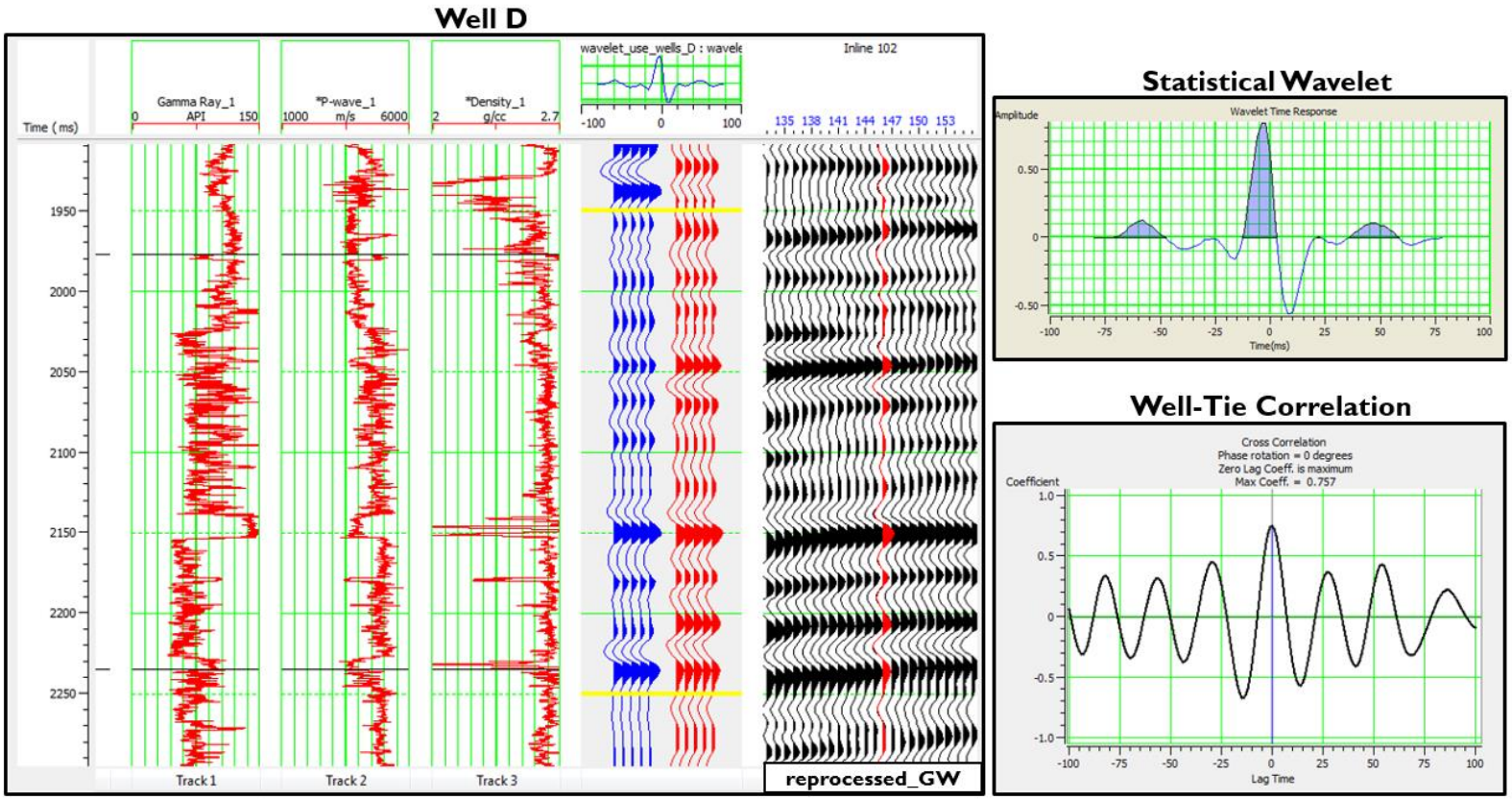

Figure 35: Density and P-wave logs, synthetic seismogram, and extracted seismic trace. There is a good correlation between the synthetic and extracted seismic traces (correlation = 0.757).

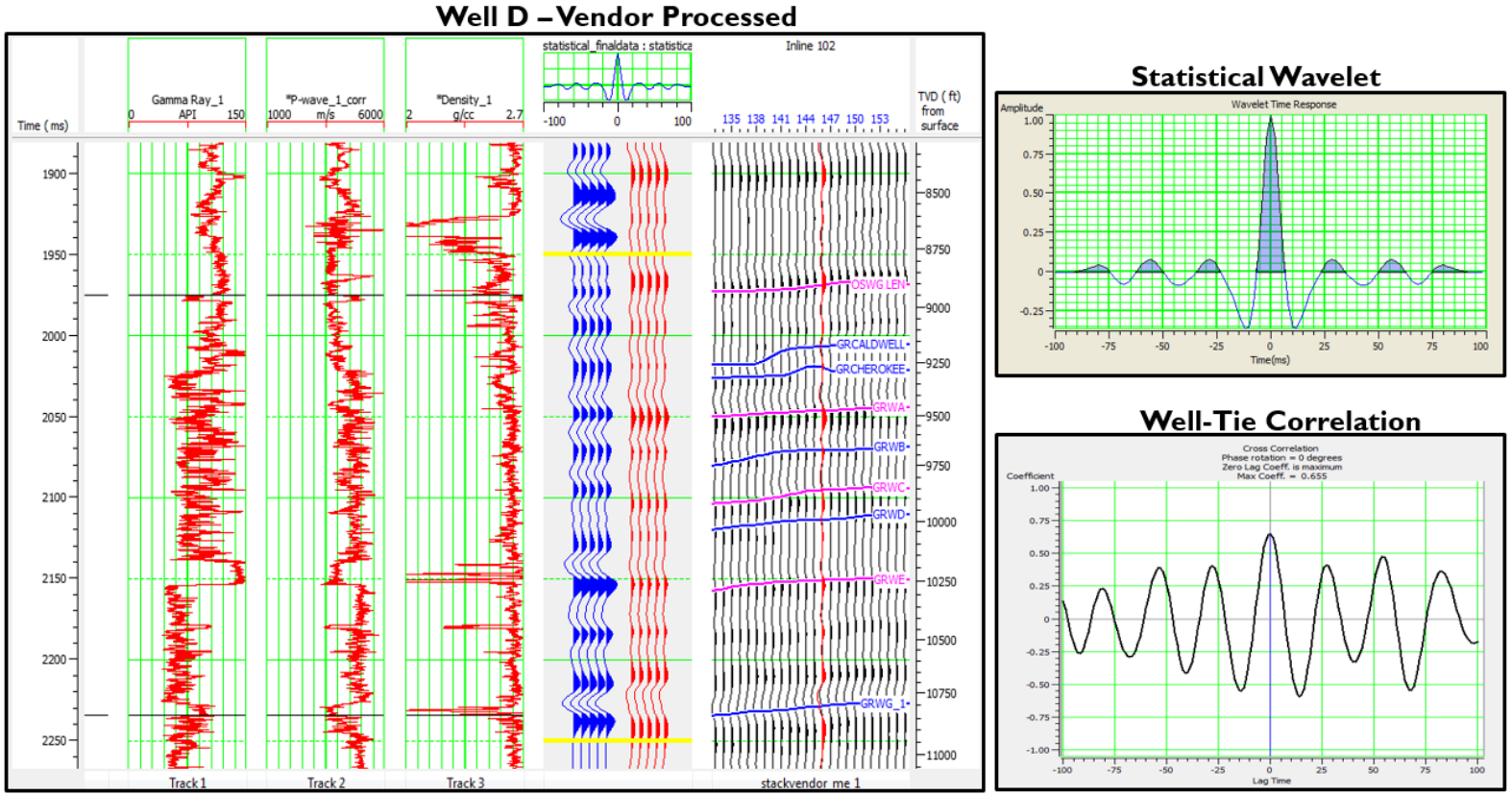

Figure 36: Density and P-wave logs, synthetic seismogram, and extracted seismic trace of the **vendor-processed** data. The correlation obtained is lower (0.655) compared to the value obtained (0.757) when the wells are tied to the reprocessed data.

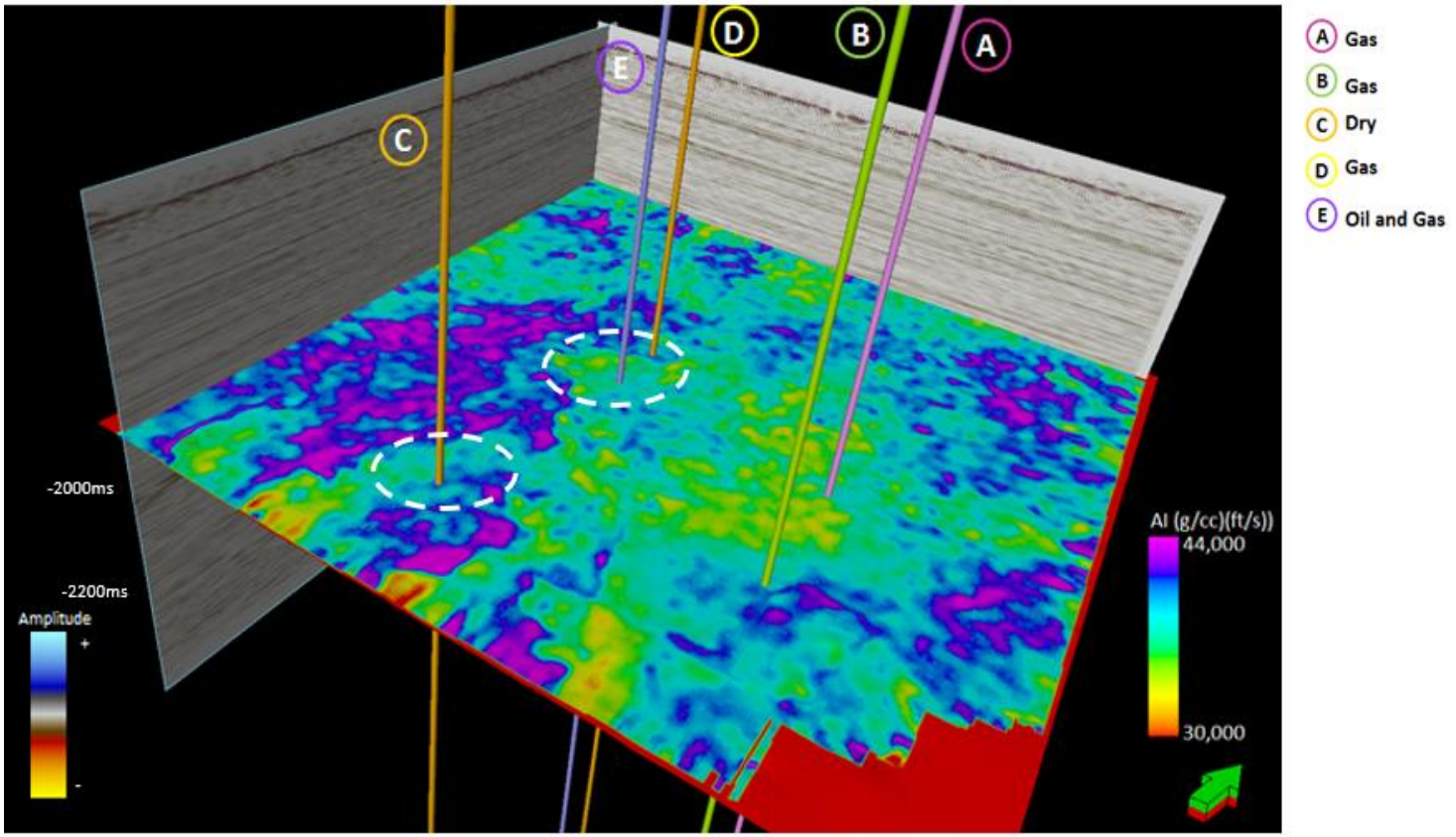

Figure 37: Acoustic impedance map extracted over the Cherokee Wash. Well C (Dry wells) correspond to a relatively high impedance value while Well E (Oil and Gas producing well corresponds to relatively low impedance values. The result is corroborated with Senoglu (2017) well logs crossplot of acoustic impedance versus porosity.

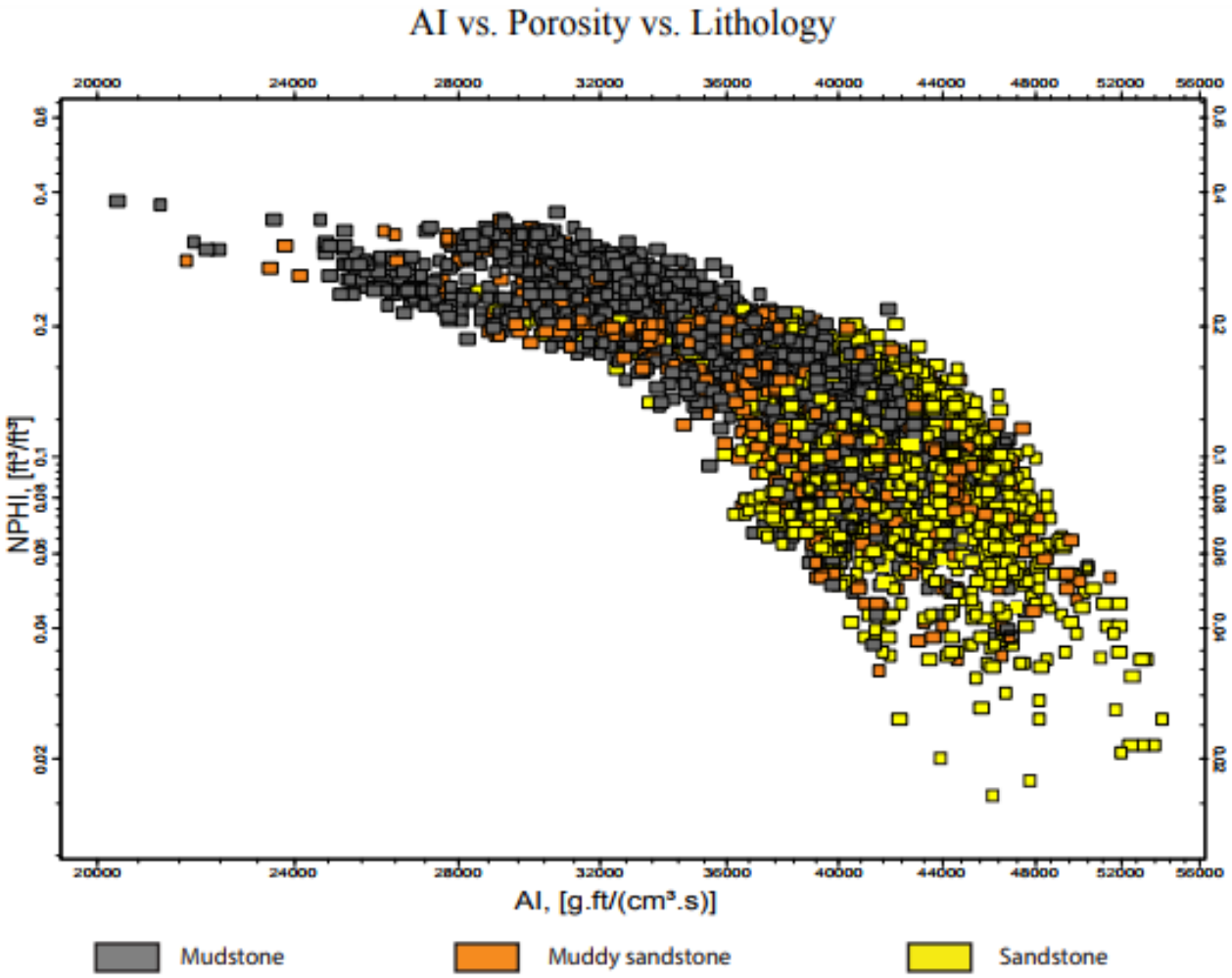

Figure 38: Well-log crossplot of acoustic impedance versus porosity and color coded by lithology showing relatively high impedance values corresponding sandstones to while moderate or low acoustic impedance values are associated with either muddy sandstone or shale (modified from Senoglu, 2017)

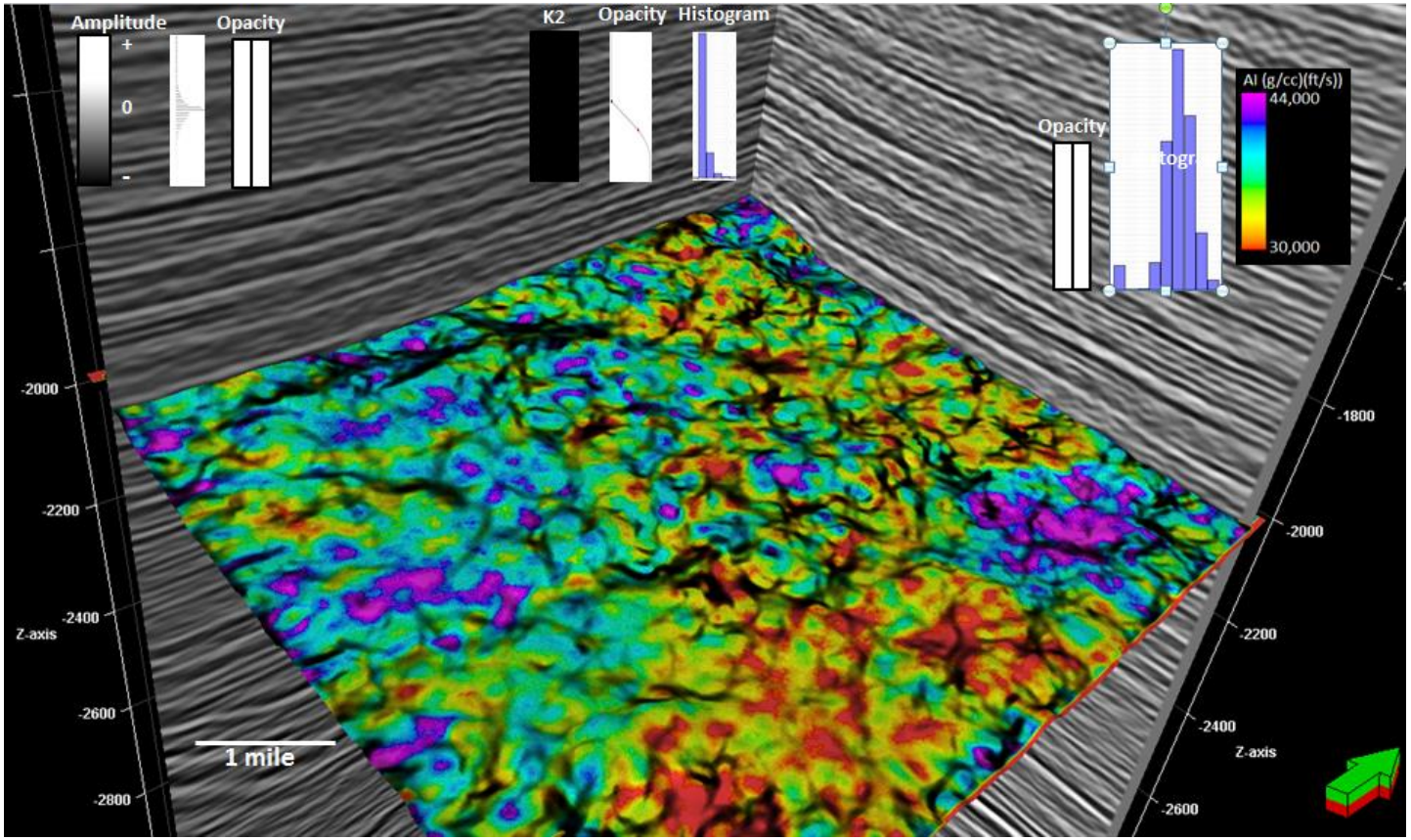

Figure 39: Post-Stack acoustic impedance inversion co-rendered with K2 most negative curvatures. Note that pockets of low AI correspond to ‘’valley’’ values of the curvature anomalies. Curvature is an indicator of strain and may be proxy for areas of high fracture density. The post stack AI is extracted along the top of the Cherokee wash.

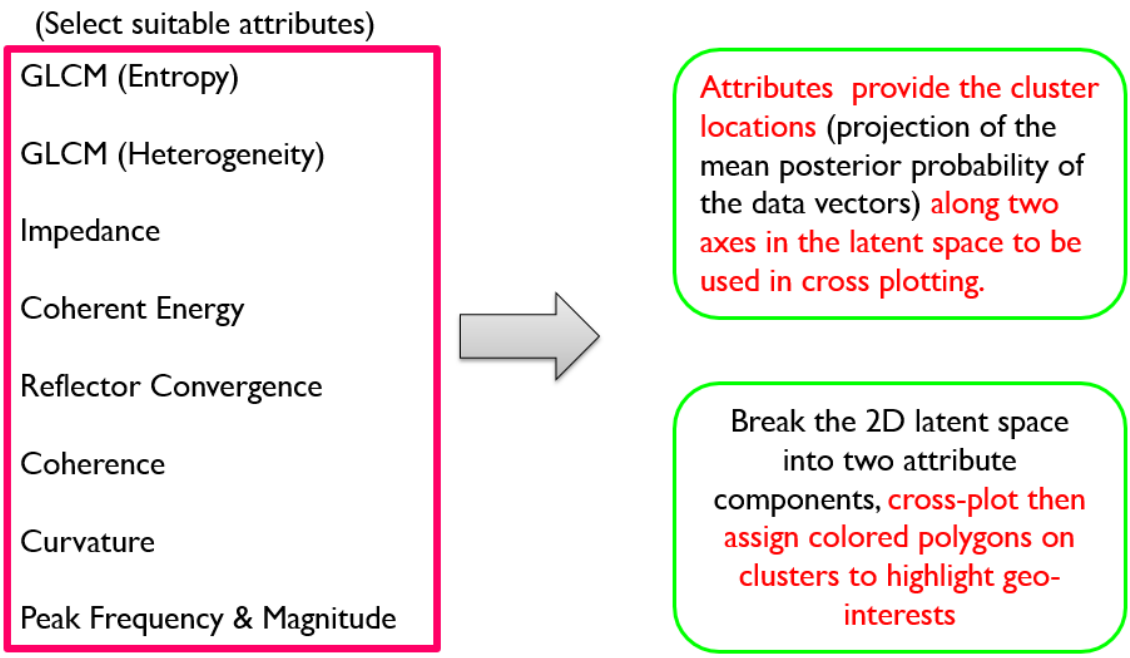

Figure 40: Graphic showing the input seismic attributes fed into our GTM algorithm.

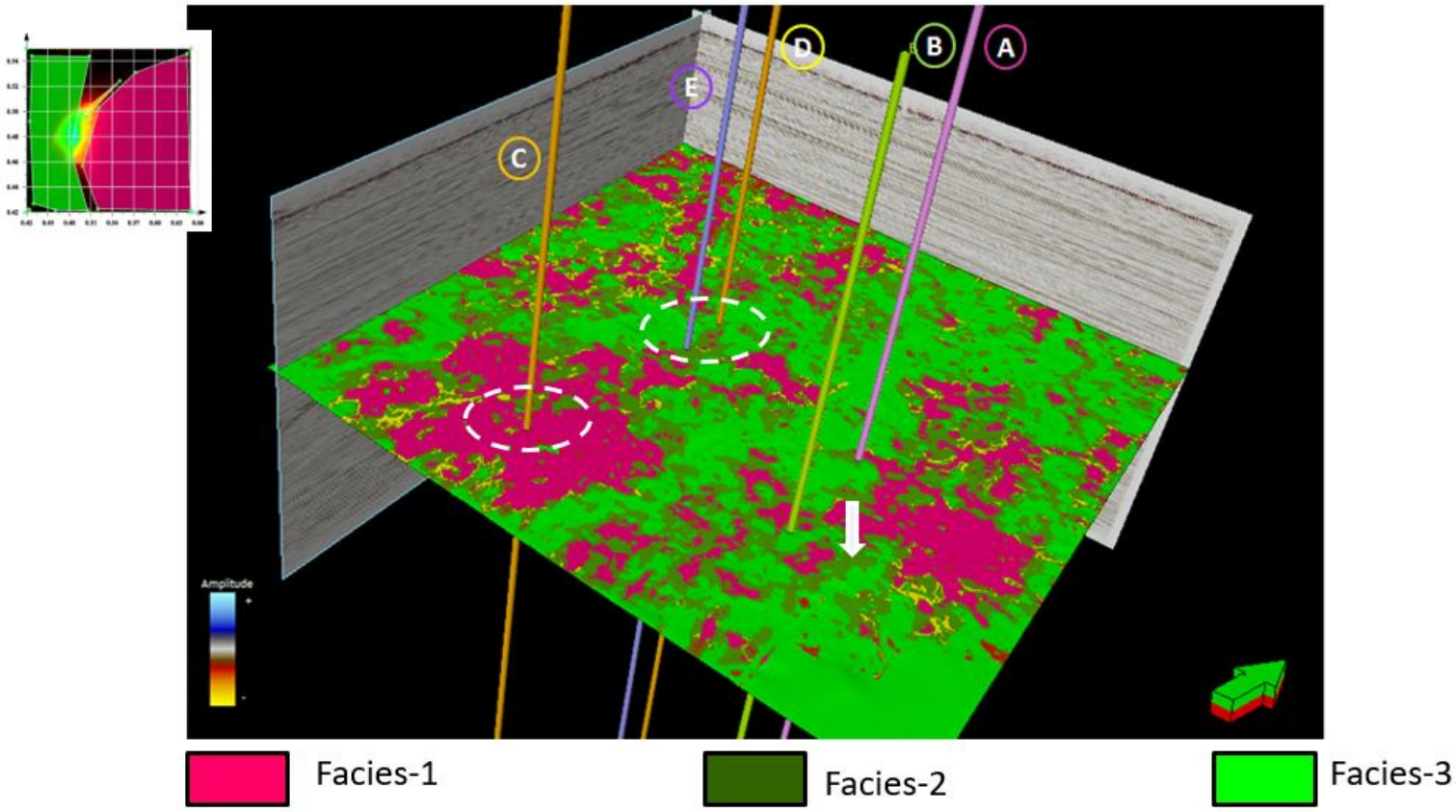

Figure 41: Facies volume from unsupervised GTM Classification (GTM3D). Input attributes are Coherence, GLCM (homogeneity), P-impedance, reflector convergence, peak frequency. Based on Senoglu's (2017) work, Facies 1 corresponds to sandstones while Facies 2 and 3 could be either muddy sandstones or mudstones.

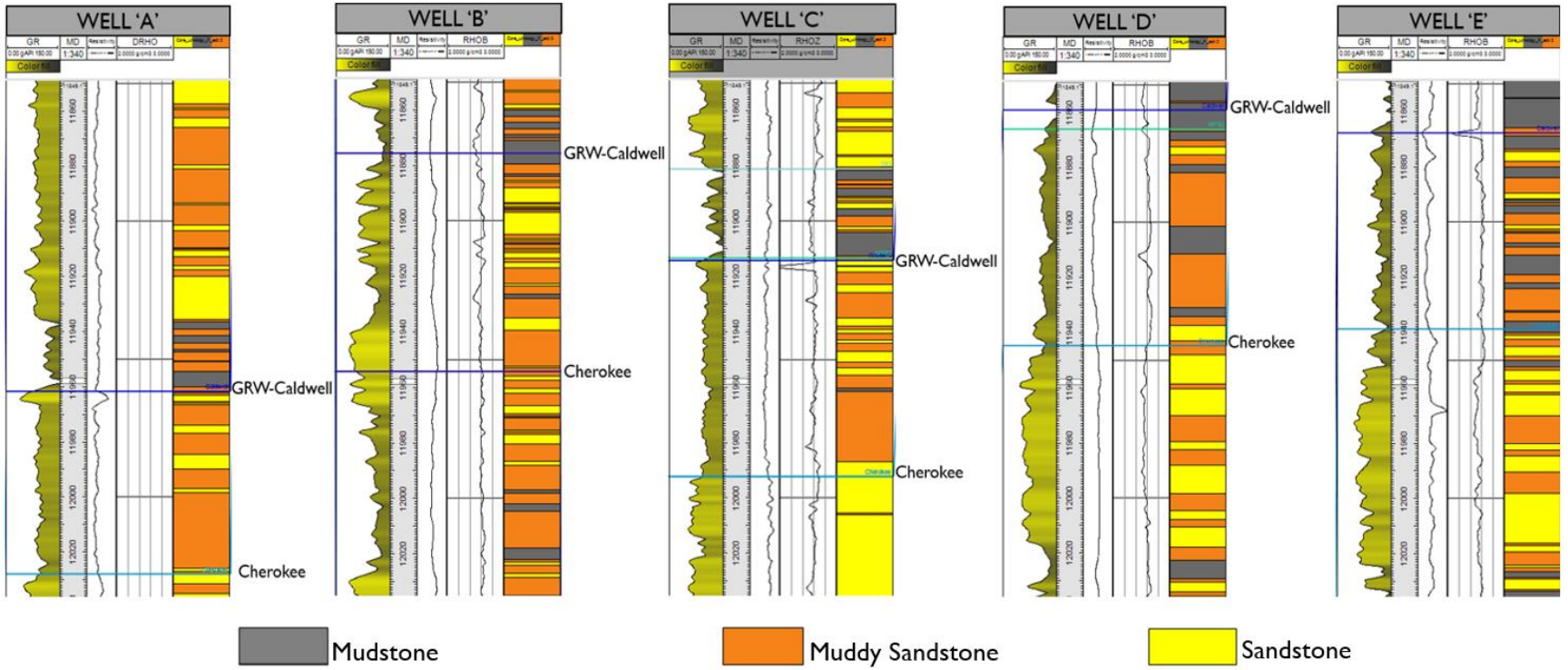

Figure 42: Well section of Wells A, B, C, D and E showing gamma-ray, resistivity and Vshale logs together with the core lithology and resultant lithology logs from combination neural network and gamma-ray cut-off methods. (Based on Senoglu's 2017 work)